**ISTANBUL TECHNICAL UNIVERSITY ★ GRADUATE SCHOOL**

# SCALABLE MECHANICAL DESIGN FOR QUADRUPED ROBOTS

**M.Sc. THESIS**

**Faraz RAHVAR**

**Department of Mechatronics Engineering**

**Mechatronics, Robotics, and Automation Engineering Programme**

**JULY 2024**

**ISTANBUL TECHNICAL UNIVERSITY ★ GRADUATE SCHOOL**

# SCALABLE MECHANICAL DESIGN FOR QUADRUPED ROBOTS

**M.Sc. THESIS**

**Faraz RAHVAR**
**(518221005)**

**Department of Mechatronics Engineering**

**Mechatronics, Robotics, and Automation Engineering Programme**

**Thesis Advisor: Assis. Prof. Dr. Abdurrahman YILMAZ**

**JULY 2024**

**ISTANBUL TEKNİK ÜNİVERSİTESİ ★ LİSANSÜSTÜ EĞİTİM ENSTİTÜSÜ**

# DÖRT AYAKLI ROBOTLAR İÇİN ÖLÇEKLENDİRİLEBİLİR MEKANİK TASARIM

**YÜKSEK LİSANS TEZİ**

**Faraz RAHVAR**
**(518221005)**

**Mekatronik Mühendisliği Bölümü**

**Mekatronik, Robotik ve Otomasyon Mühendisliği Programı**

**Tez Danışmanı: Dr. Öğr. Üyesi Abdurrahman YILMAZ**

**JULY 2024**

Faraz-Rahvar, a M.Sc. student of ITU Graduate School student ID 518221005, successfully defended the thesis/dissertation entitled “SCALABLE MECHANICAL DESIGN FOR QUADRUPED ROBOTS”, which he prepared after fulfilling the requirements specified in the associated legislations, before the jury whose signatures are below.

**Thesis Advisor :** **Assis. Prof. Dr. Abdurrahman YILMAZ** .....
Istanbul Technical University

**Jury Members :** **Prof. Dr. Hakan TEMELTAS** .....
Istanbul Technical University

**Assis. Prof. Dr. Fatih ADIGUZEL**
Yildiz Technical University

**Date of Submission : 20.05.2024**
**Date of Defense : 10.07.2024**

***To my Iran and Türkiye,***

**FOREWORD**

I am truly grateful to my advisor, Assistant Professor Dr. Abdurrahman Yilmaz, for his valuable support and guidance throughout my Master's program at ITU. His kindness, empathy, and unwavering support have been greatly appreciated.

Additionally, I owe a profound debt of gratitude to my family. Their love, sacrifices, and constant support throughout my life have shaped me into the person I am today. Without their endless contributions, I would not be where I am now.

May 2024 Faraz RAHVAR

**TABLE OF CONTENTS**

**Page**

## ABBREVIATIONS

**CNN** : Convolutional Neural Network
**COT** : Cost of Transport
**MCOT** : Mechanical Cost of Transport
**MP** : Mechanical Parameter
**QDD** : Quasi Direct Drive
**QR** : Quadruped Robot
**RL** : Reinforcement Learning
**SCA** : Scalable Control Architecture
**SDF** : Signed Distance Function
**SMD** : Scalable Mechanical Design
**ZMP** : Zero Moment Point

**SYMBOLS**

| | |
|---|---|
| **Ej** | **:** Joule Heating |
| **I** | **:** Electrical Current |
| **$K_M$** | **:** Motor Constant |
| **R** | **:** Motor Terminal Resistance |

## LIST OF TABLES

**Page**

**LIST OF FIGURES**

**Page**

## SCALABLE MECHANICAL DESIGN FOR QUADRUPED ROBOTS

## SUMMARY

Nowadays, the vital role of robots in human life is not only undeniable, but it is also essential. Quadruped robots, in particular, which mimic four-legged animals, have been significantly crucial in emergency and critical situations. In this thesis, we deeply focused on different mechanical parameters affecting the design of quadruped robots while considering the dimensional scaling of both robot parts and trajectory length and height, thereby potentially leading us to achieve a scalable control architecture for Quadruped Robots (QRs).

The scalability of QRs can significantly enhance their capabilities. If a QR can adjust its size, it can quickly conceal itself under debris to observe enemy operations or navigate through narrow pathways under earthquake rubble. Achieving this ability necessitates a scalable mechanical design, which in turn requires a scalable control architecture. Such an architecture relies heavily on mechanical parameters. To realize this scalable control architecture, it is imperative to meticulously monitor the behavior of these parameters and establish relationships among them.

In this thesis, we conducted simulations involving a standard commercial quadruped robot, Unitree A1, walking on a flat surface at a constant speed across five distinct scenarios. Given that contemporary quadruped robots typically feature four motors in the hips and four in the elbows, our simulation followed this configuration, employing a total of eight motors. We just focused on walking forward direction. So lateral movements and turning and other disturbance rejection capabilities are ignored.

There are four different sizes of the robot, each expanding the robot size by 30%. In the first scenario, we define the length and height of the trajectory as 120 mm and 27 mm, respectively to observe the effect of scaling. In the second scenario, we increased the length of the trajectory from 120 mm to 165 mm to observe the effect of length increase in trajectory. Then in the third scenario, we defined the length of the trajectory as 165 mm while increasing the height of the trajectory from 27 mm to 40 mm to observe the effect of the step height increase. The fourth scenario maintains the same trajectory length and height as the second scenario, and robot scaling remains consistent except for the Torso to observe the effect of Torso. The Torso retains the dimensions of the Torso of the fourth robot in scenario two (the longest). The linear velocity in all scenarios is 250 mm/s and the robots walk on a flat terrain.

Due to the unavailability of precise dimension drawings of the Unitree A1 robot, we endeavored to design its various components in CATIA software, approximating existing robot dimensions. Subsequently, the parts were assembled using SolidWorks software. Leveraging the motion analysis tool within SolidWorks, our thesis aims to generate diverse outcomes, including motor torque, power consumption of the motors, reaction forces, motor angular displacements, linear velocity of the robots, and the mechanical cost of transport (MCOT). By comparing these outcomes, our goal is to establish logical relationships among the mechanical parameters of a standard commercial quadruped robot. The findings of this study hold implications for various actuation design architectures, such as Quasi Direct Drive (QQDs) and series elastic robots. They provide valuable insights that can inform the development and optimization of such architectures while scaling.

In conclusion, to the best of our knowledge, there have been no studies examining changes in the mechanical principles of quadruped robots during scaling. Quadruped robots are highly effective in specialized tasks, especially in disaster scenarios like earthquakes, where their mobility outperforms fixed robots. However, altering the dimensions of these robots significantly affects their mechanical and control requirements. This study examined key mechanical parameters, including hip and calf torque, power consumption, reaction forces, and mechanical cost of transport across five different scaling scenarios using simulations with a Unitree A1 quadruped robot. The simulations revealed that while the behavioral patterns of the robots remained consistent, the mechanical demands increased with the elongation of the torso, arms, and legs. Significant changes in angular velocity and displacement of limbs were observed, correlating with motor performance. Successful scaling depends on the motors' ability to handle maximum torque and power consumption requirements while maintaining necessary angular velocity. The study found a consistent mechanical cost of transport (MCOT) across scenarios, with a decrease as trajectory length and height increased, highlighting the importance of minor mechanical variations on energy efficiency. These results provide valuable insights for designing various actuator architectures, not limited to a single actuator type, thereby enhancing their applicability. The research identifies a clear pattern of torques, power consumptions, and reaction forces as the robots scale in size. Future research aims to use this data to develop a scalable control architecture, integrating machine learning. Our research elucidates the behavior of these mechanical parameters during scaling, thereby offering a novel perspective on scalable control architecture in quadruped robots. On the other hand, in scenario five, only the Torso is scaled while the arms and legs retain the dimensions of robot three in scenario two.

# DÖRT AYAKLI ROBOTLAR İÇİN ÖLÇEKLENDİRİLEBİLİR MEKANİK TASARIM

## ÖZET

Dört ayaklı robotlar, özellikle hareket kabiliyetlerinin sabit robotlardan daha üstün olduğu deprem gibi afet senaryolarında özel görevler için vazgeçilmezdir. Bununla birlikte, bu robotların boyutlarının değiştirilmesi, mekanik gereksinimleri ve kontrol sistemlerini önemli ölçüde etkiler. Bu çalışma, ölçeklenebilirliğin farklı boyutlardaki tasarımlar üzerindeki etkilerini anlamayı amaçlayarak, ölçeklendirme sürecinde dört ayaklı robotların kontrol sistemlerini etkileyen temel mekanik parametreleri araştırmakta ve karşılaştırmaktadır. Standart bir yarı doğrudan tahrikli ticari dört ayaklı robot modeli kullanılarak, her biri robot boyutunu %30 oranında genişleten dört farklı boyutta simülasyonlar gerçekleştirilmiştir. Bu simülasyonlar, robot düz bir yüzey üzerinde sabit bir hızda yürürken statik ve dinamik kuvvetleri analiz etmektedir. Özellikle, gerekli tork, robot motorlarının enerji tüketimi, robot ayakları ile zemin arasındaki reaksiyon kuvvetleri ve taşımanın mekanik maliyeti incelenmektedir. Bu sonuçlar, eklemler de dahil olmak üzere mekanik analiz perspektifinden robotun kritik bileşenlerini kapsar ve çeşitli aktüatör mimarisi tasarımları için değerli referanslar sağlar. Bulgularımız, robot ölçeklendikçe tork, güç tüketimi ve reaksiyon kuvvetlerinin artışında mantıklı bir model ortaya koymaktadır. Bu içgörüler, bacaklı robotlar için ölçeklenebilir bir kontrol mimarisi geliştirmeye zemin hazırlamaktadır. Günümüzde robotların insan yaşamındaki hayati rolü yadsınamaz ve gereklidir. Özellikle dört ayaklı hayvanları taklit eden dört ayaklı robotlar, acil ve kritik durumlarda önemli roller üstlenmektedir. Bu tezde, hem robot parçalarının hem de yörünge uzunluğu ve yüksekliğinin boyutsal ölçeklendirmesini göz önünde bulundurarak dört ayaklı robotların tasarımını etkileyen farklı mekanik parametrelere derinlemesine odaklandık ve böylece potansiyel olarak Dört Ayaklı Robotlar (QR'ler) için ölçeklenebilir bir kontrol mimarisi elde ettik. QR'lerin ölçeklenebilirliği yeteneklerini önemli ölçüde artırabilir. Bir QR boyutunu ayarlayabilirse, düşman operasyonlarını gözlemlemek için enkaz altında kendini gizleyebilir veya deprem enkazı altındaki dar yollarda gezinebilir. Bu kabiliyetin elde edilmesi, ölçeklenebilir bir mekanik tasarım ve ölçeklenebilir bir kontrol mimarisi gerektirir. Bu tür bir mimari büyük ölçüde mekanik parametrelere dayanır. Bu ölçeklenebilir kontrol mimarisini gerçekleştirmek için, bu parametrelerin davranışlarını titizlikle izlemek ve aralarında ilişkiler kurmak zorunludur. Bu tezde, standart bir Unitree A1 robotunun düz bir yüzey üzerinde sabit bir hızda beş farklı senaryoda yürümesini içeren simülasyonlar gerçekleştirdik. Çağdaş dört ayaklı robotların tipik olarak kalçalarda dört ve dirseklerde dört motora sahip olduğu göz önüne alındığında, simülasyonumuz toplam sekiz motor kullanarak bu konfigürasyonu takip etti. Robotların uzunluğu, ilk üç senaryo boyunca birinci robottan dördüncü robota kadar 0,3 katsayısı ile kademeli olarak artırılmıştır. İkinci ve üçüncü senaryolarda, yörüngenin uzunluğu ve yüksekliği sırasıyla artırılmıştır. Buna karşılık, dördüncü ve beşinci senaryolarda sırasıyla kollar ve bacaklar ile gövde ölçeklendirilirken yörüngenin boyutları korunmuştur. Bir

standart dört ayaklı robotunun kesin boyut çizimlerinin mevcut olmaması nedeniyle, çeşitli bileşenlerini mevcut robot boyutlarına yaklaşarak CATIA yazılımında tasarlamaya çalıştık. Daha sonra parçalar SolidWorks yazılımı kullanılarak birleştirildi. SolidWorks'teki hareket analizi aracını kullanan tezimiz, motor torku, motorların güç tüketimi, reaksiyon kuvvetleri, motor açısal yer değiştirmeleri, robotların doğrusal hızı ve mekanik taşıma maliyeti (MCOT) dahil olmak üzere çeşitli sonuçlar üretmeyi amaçlamaktadır. Bu sonuçları karşılaştırarak, amacımız ölçeklendirilmiş standart dört ayaklı robotun mekanik parametreleri arasında mantıksal ilişkiler kurmaktır. Bu çalışmanın bulguları, Quasi Direct Drive (QQDs) ve seri elastik robotlar gibi çeşitli aktüatör tasarım mimarileri için çıkarımlar içermektedir. Ölçeklendirme sırasında bu tür mimarilerin geliştirilmesi ve optimizasyonu hakkında bilgi verebilecek değerli içgörüler sağlarlar. Bildiğimiz kadarıyla, ölçeklendirme sırasında dört ayaklı robotların mekanik prensiplerindeki değişiklikleri inceleyen herhangi bir çalışma bulunmamaktadır. Araştırmamız, ölçeklendirme sırasında bu mekanik parametrelerin davranışını aydınlatmakta ve böylece dört ayaklı robotlarda ölçeklenebilir kontrol mimarisine yeni bir bakış açısı sunmaktadır. Bu çalışmada, robotu ölçeklendirirken QR'lerin kontrol sistemlerini etkileyen mekanik parametrelere ulaşmaya ve bunları karşılaştırmaya odaklanıyoruz. Bu amaçla, standart bir QR'ye etki eden tüm statik ve dinamik kuvvetleri analiz ettik. Bu verilerin elde edilmesiyle robot motorlarının gerekli tork ve enerjisi belirlenebilmektedir. Bu temel sonuçlar, bizi tüm QR'lere uygulanabilir bir kontrol algoritması geliştirmeye yöneltti. Bu araştırmanın sonuçları, farklı ölçeklerdeki ölçeklenebilir robotların verilerini ve fiziksel davranışlarını karşılaştırarak, kontrol bilimi alanındaki araştırmacıları, tüm QR'lerde uygulanabilecek QR'lerin SCA'sındaki ilerlemelere yönlendirebilir. Robotlar, örneğin depremlerde özel görevlerini yerine getirmek için sabit robotlara kıyasla ölçeklenebilme kabiliyetiyle çok faydalı yeteneklere sahip olabilirler. Elbette robotun boyutlarının değiştirilmesiyle robotu hareket ettirmek için gereken tork miktarı ve robota etki eden dinamik ve statik kuvvetler değişecektir. Bu değişiklikler robotun kontrolü üzerinde önemli bir etkiye sahiptir. Kontrol sistemine uygulanabilir ölçeklenebilir bir model oluşturmak için bu fiziksel değişikliklerden kaynaklanan çıktı verilerini farklı ölçeklerde hesapladık. Dört ayaklılar köpek, kedi, at ve deve gibi dört ayaklı hayvanlardır. Robotikte QR'ler, dört ayaklı bir hayvanın hareketini taklit edecek şekilde hareket etmek üzere tasarlanmış dört ayaklı biyolojik olarak esinlenmiş robotlardır. QR'ler genellikle zorlu arazilerden geçme, ağır yük taşıma veya insanlar için tehlikeli olan ortamlarda görev yapma gibi belirli hedefler göz önünde bulundurularak tasarlanır. Bu tezi yürütmek için gerekli motivasyon, QR'lere kontrol ve mekanik tasarım uygulamak için bir model elde etmektir. Başka bir deyişle, bu robotların mekanik tasarımında ölçeklenebilirlik sağlanarak, farklı boyutlardaki QR'lere uygulanabilir bir kontrol sistemi tasarlamak amacıyla kabul edilebilir bir model elde edilebilir. Bu yaklaşım, robota çeşitli durumlarda uygulanan dinamik ve statik analizlerin sonuçlarının robotun boyutlandırılması ve kontrolü için değerli veriler olarak kullanılmasını sağlar. Bu amaçların yerine getirilmesiyle, bu çalışmanın önemli pratik ve bilimsel etkileri olabileceği gibi, en ileri robotik teknolojisinin geliştirilmesine de katkıda bulunabilir. Dört ayaklı robotlar, özellikle felaket senaryolarında, hareket kabiliyetlerinin genellikle statik gövdeli robotlardan daha iyi performans gösterdiği özel görevler için paha biçilmez yetenekler sergilemektedir. Ancak, bu robotların boyutlarının değiştirilmesi mekanik gereksinimlerini ve kontrol sistemlerini önemli ölçüde etkilemektedir. Bu çalışma, kalça ve baldır torku, kalça ve baldır güç tüketimi, uç efektör ile zemin arasındaki reaksiyon kuvvetleri ve ölçeklendirilmiş robotların üç

farklı senaryoda taşınmasının mekanik maliyeti dahil olmak üzere temel mekanik parametreleri araştırmayı ve karşılaştırmayı amaçlamıştır. Amacımız, bunların ölçeklendirme sırasında dört ayaklı robotların dinamikleri üzerindeki etkilerini gözlemlemektir. Başka bir deyişle, bu robotların mekanik tasarımında ölçeklenebilirlik sağlanarak, farklı boyutlardaki QR'lere uygulanabilir bir kontrol sistemi tasarlamak amacıyla kabul edilebilir bir model elde edilebilir. Bu yaklaşım, robota çeşitli durumlarda uygulanan dinamik ve statik analizlerin sonuçlarının robotun boyutlandırılması ve kontrolü için değerli veriler olarak kullanılmasını sağlar. Bu amaçların yerine getirilmesiyle, bu çalışmanın önemli pratik ve bilimsel etkileri olabileceği gibi, en ileri robotik teknolojisinin geliştirilmesine de katkıda bulunabilir. Dört ayaklı robotlar, özellikle felaket senaryolarında, hareket kabiliyetlerinin genellikle statik gövdeli robotlardan daha iyi performans gösterdiği özel görevler için paha biçilmez yetenekler sergilemektedir. Ancak, bu robotların boyutlarının değiştirilmesi mekanik gereksinimlerini ve kontrol sistemlerini önemli ölçüde etkilemektedir. Bu çalışma, kalça ve baldır torku, kalça ve baldır güç tüketimi, uç efektör ile zemin arasındaki reaksiyon kuvvetleri ve ölçeklendirilmiş robotların üç farklı senaryoda taşınmasının mekanik maliyeti dahil olmak üzere temel mekanik parametreleri araştırmayı ve karşılaştırmayı amaçlamaktadır. Amacımız, bunların ölçeklendirme sırasında dört ayaklı robotların dinamikleri üzerindeki etkilerini gözlemlemektir.

# 1. INTRODUCTION

Quadrupeds are animals with four legs, such as dogs, cats, horses, and camels. In robotics, QRs are biologically inspired robots that have four legs that are designed to move in a way that mimics the locomotion of a quadrupedal animal. QRs are often designed with specific goals in mind, such as the ability to traverse challenging terrain, carry heavy loads, or perform tasks in environments that are hazardous to humans.

## 1.1 Research Topics On Quadruped Robots

QRs have been a topic of interest to researchers in recent years, and many research groups are working in this area. Many topics can be explored in the field of QRs, such as:

- Gait analysis: The study of the movement patterns of quadruped animals and how these can be replicated in robots. This includes research on different types of gaits, such as bounding, trotting, and galloping.
- Design optimization: Research on how to optimize the design of QRs for specific applications, such as search and rescue, transportation, and exploration.
- Control systems: Development of advanced control systems for QRs, including the use of control theory and artificial intelligence techniques. Since QRs are unstable systems, controlling such structures is challenging and crucial.
- Actuator systems: Research on how to design special actuator systems for QRs. There are various types of QRs in terms of actuation. Different types of actuators are used to provide movement in the joints and these actuators can be placed on the robot in different architectures.
- Sensing and perception: Research on how to improve the sensing and perception capabilities of QRs, including the use of sensors such as lidar, cameras, IMU, and microphones.

- Mobility in challenging terrain: Exploration of how QRs can be designed to navigate challenging terrain, such as rocky or uneven surfaces, steep slopes, and soft soils.
- Human-robot interaction: Investigation of how QRs can interact with humans and other robots in a variety of settings, including urban environments, disaster zones, and manufacturing facilities.
- Multi-robot systems: Exploration of how QRs can work as a team to achieve complex tasks, such as cooperative transportation, mapping, or search and rescue missions.

Quadruped Robots can have very useful capabilities to perform their special missions in earthquakes, for instance, with the ability to scale compared to fixed robots. Certainly, by changing the dimensions of the robot, the amount of torque required to move the robot and the dynamic and static forces acting on the robot will change. These changes have a significant impact on the control of the robot.

### 1.2 Hypothesis and Purpose of Thesis

In this study, we focus on reaching and comparing mechanical parameters affecting the control systems of QRs while scaling the robot. For this purpose, we analyzed all the static and dynamic forces acting on a standard QR. By obtaining this data, the required torque and energy of the robot motors can be determined. We calculated the output data resulting from these physical changes in different scales to create a scalable model applicable to the control system. These fundamental outcomes lead us to develop a control algorithm applicable to all QRs. By comparing the data and physical behaviors of scalable robots in different scales, the outcomes of this research can guide researchers in the field of control science towards advancements in the Scalable Control Architecture (SCA) of QRs that can be implemented in all QRs.

The aims of the study are listed as follows:

- Develop a better understanding of the design criteria for QRs.
- Evaluate the performance of different quadruped designs (in terms of leg size, torso size, body size, etc.).

- Contribute to the development of new robotics technologies that could have practical applications in areas such as search and rescue, exploration, agriculture, and/or entertainment.

The necessary motivation for carrying out this thesis is to obtain a model for applying control and mechanical design to QRs. Designing a QR involves several crucial considerations, including the number and placement of joints, the utilization of sensors and actuators for control, the size of the body, legs, and torso, and the selection of materials for the body and leg. In other words, by achieving scalability in the mechanical design of these robots, an acceptable model can be obtained with the aim of designing a control system applicable to QRs of different sizes. This approach enables the results of dynamic and static analyses applied to the robot in various situations to be used as valuable data for sizing and controlling the robot. By meeting these aims, this study could have significant practical and scientific implications, as well as contribute to the development of cutting-edge robotics technology.

## 2. LITERATURE REVIEW

In this section, we review previous studies on quadruped robots, considering the top contributions from both recent and past research. Section 3.2 outlines our general hypotheses, while section 3.3 provides details on our scaling plans. Section 4 delineates the simulation steps and methodologies. Within this section, we compare the behaviors of mechanical parameters across different scales of the robot, illustrating how scaling impacts these principles. Finally, in section 5, we conclude our study and discuss avenues for future research related to scaling.

### 2.1 Energy Efficiency

While implementing the design principles for highly efficient legged robots, considering energy efficiency is one of the most effective factors. The total cost of transport( TCoT) is the most common tool to measure the energy efficiency of legged robots (Bhounsule, 2012). Given the notable energy disparity between legged robots and creatures traversing flat surfaces, efforts continuously continue to enhance energy efficiency in the realm of legged robots. The Cornell Ranger could achieve a TCoT of 0.19 using the passive dynamic walking concept, which is one of the mechanical energy capacitors, to improve energy consumption by storing the kinetic or elastic potential energy (Bhounsule, 2012; Tedrake R. a.-f., 2004). Series elastic actuators are further mechanical energy capacitors that recorded a TCoT of 1.7 for iSprawl (Hurst, 2010; Hutter, 2012; Wolf, 2008). Electromagnetically actuated robots often encounter limitations in their mechanical transmission systems, especially within the interface of the electric motor and the robot's extremities, Series Elastic Actuators (SEA) strategically integrate a spring at the actuator's endpoint to alleviate impact loads on transmissions and enable torque control in a closed-loop manner. On the flip side, robots like the MIT Cheetah rely on internal adaptability within their mechanisms, connections, and feet to effectively regulate and minimize abrupt external pressures. (Williamson, 1995; Katz, 2019).Using parallel mechanical springs as outlined in (Folkertsma, 2012) and integrating morphological computation represent additional

mechanisms for storing mechanical energy, resulting in a 53% decrease in overall power usage and leveraging the inherent dynamics of the robot for legged movement, respectively (Iida, 2005; Zhao, 2012). The design concept of co-locating tendons and bones has potential implications for enhancing the efficiency of running concerning energy. This occurs due to the potential for utilizing the saved energy in the tendon while in contact with the terrain to boost acceleration during takeoff (Ananthanarayanan, 2012). While these methods only focus on mechanical energy losses, we should take a look at the fundamentals in the structure of the MIT Cheetah to consider the nonmechanical energy losses. The first loss in an electromagnetic motor is Ej ( Ej = $\int I^2 Rdt$) at the force transducer. The second loss is in transmission which is called $E_f$ and encompasses all energy dissipations along force transmission routes, such as losses from friction in bearings, gears, and belts. Foot impact and air drag are the significant sources of energy loss referring to the third form of energy dissipation known as mutual loss. Since the continuous torque of an electromagnetic motor is closely associated with the constant of the motor, $K_{M,}$ ( $K_M = \tau / \sqrt{I^2 R}$) using electromagnetic motors with high torque per unit volume can reduce Ej by 75% provided that other factors, such as the mass of motor and thermal dissipation properties, do not vary (Seok S. a., 2014). Additionally, one of the underlying measures of these motors' performance is gap radius: the distance between the windings of the motor stator and the permanent magnets attached to the rotor (Seok S. a., 2012). Sangok et al. have demonstrated that within a model framework where the mass of the motor and uninterrupted torque demand remains constant, while the gap radius is allowed to change and massless, frictionless gear trains are introduced to fulfill torque requirements, the resulting output torque and total reflected inertia remain unaffected by the gap radius and corresponding gear ratio. This finding suggests that an analysis incorporating gear inertia and friction would favor motors with larger gap radii, as they entail smaller gear ratios and fewer gear-train stages. Consequently, this configuration yields reduced friction loss, enhanced torque density, and increased bandwidth. Regarding these insights, utilizing a bespoke three-phase synchronous motor enhances the motor's continuous torque density by approximately 1.5 times compared to the commercial motor employed in MIT Cheetah (Seok S. a., 2014). During the initial ground phases and the final swing phase, the legs perform negative work, with torques and angular velocities opposing each other. Much like regenerative

braking in electric vehicles, it's preferable to recuperate this energy rather than dissipating it through dampers and brakes (Ruina, 2005; Yoong, 2010). An alternative approach to recovering this energy involves implementing virtual impedance through electromagnetic torque control at the actuators, replacing the need for mechanical springs, dampers, and series elastic actuation. Enhancing the efficiency of power generation can also be achieved through a power transmission path with reduced impedance (Seok S. a., 2014). The motor driver on the MIT Cheetah robot is designed for energy regeneration, acting as a generator during negative work phases (Yoong, 2010; Torres, 2015). It employs custom switching converters and pulse-width modulation to control torque production and battery charging. Efficiency tests reveal dominant Joule heating and FET switching losses. Experimental results confirm successful battery recharging during simulated running impacts, with 63% of negative mechanical work recovered. Steady-state running redistributes regenerated energy among motors, maintaining battery power at or above zero (Salameh, 2009; Seok S. a., 2014). Slender legs are advantageous for fast-paced locomotion due to the low inertia of the leg, reducing torque demands during the swing phase, particularly in high-acceleration phases like protraction. Low inertia legs enable faster swing motion and shorter swing phases, allowing for a larger duty factor at a given running speed (Weyand, 2000). The preservation of vertical momentum theory suggests that shorter swing times during running minimize the required vertical momentum with every stride. The reduction occurs due to shorter durations of the swinging phase resulting in abbreviated running cycles, decreasing the loss of vertical momentum due to the gravitational force experienced with each step during consistent running. Consequently, a larger duty factor, which extends the leg's contact time with the ground, can mitigate the peak ground reaction force. This reduction in ground reaction force corresponds to decreased energy usage, as it decreases the torque required from the motors (Haberland, 2011; Seok S. a., 2014). By implementing the four principles of legged robot design, Seok et al. could lead the MIT Cheetah to a COT equivalent to 0.5, a measure comparable to that observed in natural running animals and notably superior to other existing running robots (Seok S. a., 2014).

### 2.2 Main Principles

In legged robots, the duration of time that the leg remains in contact with the ground while running is called the duty factor. The ground reaction force correlates directly

with the duty factor during running. During consistent running, the overall force exerted on the ground over one cycle must equal the force of gravity to maintain momentum balance. High-speed legged robots, typically, require a low duty factor, and bigger stride frequency (Maes, 2008). To achieve a higher stride frequency during running, it is essential to swiftly extend the leg throughout the swing phase. This rapid movement is necessary because the leg must change direction twice while in the air, transitioning from ground stroke to protraction and then to retraction. Such changes demand significant accelerations and decelerations of the leg to maintain a cyclic trajectory. This is possible by the increase in the actuator capacity and decrease in the leg inertia. In robotics, boosting actuator capacity leads to greater actuator mass, which in turn raises the demands for leg strength and leg masses. Therefore, it's preferable to choose the alternative of reducing the total inertia of the leg structure while maintaining its strength. This includes implementing one or a combination of some techniques such as: positioning the actuators nearer to the body, employing a leg design that is under-actuated, incorporating a compliant joint, and utilizing series-elastic actuation techniques using mechanical compliance to reduce the leg impedance. An alternative strategy to address the balance between strength and weight involves employing materials with high strength-to-weight ratios. Additionally, the use of tubular elements, particularly in high-speed robots, is prevalent. Integrating the tendon into a single-leg prototype resembling the limb of the MIT Robotic Cheetah, featuring an active shoulder and elbow, alongside a passive ankle and two distinct brushless DC motors close to the shoulder, aligns the leg structure more closely with a pin-jointed configuration. This adaptation results in a reduction in leg stress by approximately 59%, primarily due to the use of the smallest permissible cross-sectional area for the foot and radius, resulting in a decrease in weight (Ananthanarayanan, 2012). The modularity and cost-effectiveness of the Mini Cheetah have accelerated progress in legged robot control systems, allowing for unrestricted hardware experimentation. Its mechanical structure and actuation strategy closely mirror those of the MIT Cheetah 3, boasting a broad range of locomotion, lightweight limbs, and easily controllable actuators without the need for torque or force sensors or series compliance. Utilizing identical, self-contained actuators for all movement axes simplifies robot design, facilitates maintenance and adjustments, and minimizes expenses by ensuring part consistency (Bledt G. a., 2018). On the other hand, there are legged robots such as the Big Dog quadruped (Raibert M. a., 2008), which require high power density and utilize

hydraulic actuators operated by a two-stroke gasoline engine. Despite their capability for true rough terrain traversability, they are not ideal for smaller robots and indoor usage (Khan, 2015). In soft terrain navigation, the difference between the rigid assumption and the actual interaction with soft surfaces can greatly affect the robot's performance and stability during locomotion. Dealing with movement across soft ground can be approached from either a control or planning standpoint (Fahmi S. a., 2020). Henze et al. employed a Whole-Body Control (WBC) strategy on TORO, relinquishing the assumption of rigid contact and adopting an energy-tank method in locomotion control. Although their method effectively balanced on compliant terrain, it was only evaluated on a single type of soft terrain while the robot remained stationary. Other adaptations to soft terrain involved integrating terrain knowledge into balancing controllers, albeit these were solely tested in simulations and for monopods (Azad, 2015; Vasilopoulos, 2018). The Compliant Contact Consistent Whole-Body Control (c3WBC) ensures contact consistency across varying terrains based on terrain compliance (Fahmi S. a., 2019). Specifically, c3WBC incorporates a soft contact model into its formulation, aided by a Terrain Compliance Estimator (TCE), an online learning algorithm providing terrain compliance estimates to the c3WBC. An adaptation algorithm named STANCE was validated on the Hydraulically Actuated Quadruped (HyQ) robot during locomotion (Fahmi S. a., 2019). In contrast to previous WBC works that were only assessed during static standing (Henze B. a., 2016; Henze B. a.-G.-S., 2018), STANCE was evaluated during dynamic locomotion. Utilizing the same contact model integrated into c3WBC, STANCE dynamically adapts to various terrain types online without pre-tuning. Unlike approaches tested on simulated monopods (Azad, 2015; Vasilopoulos, 2018), STANCE was implemented and experimentally tested on the HyQ. STANCE consists of two primary modules: c3WBC and TCE. The c3WBC extends previous WBC implementations (sWBC) (Fahmi S. a., 2019) to ensure contact consistency across compliant terrains. The TCE provides online estimates of terrain compliance, closing the loop with the c3WBC. Unlike prior WBC works, STANCE does not assume rigid ground conditions. STANCE exhibits computational efficiency and overcomes limitations of previous cutting-edge methods, enabling efficient traversal across diverse terrains with varying compliances (Fahmi S. a., 2020). Employing re-planning strategies and implementing real-time Nonlinear Model Predictive Control in legged locomotion on an 87 kg Hydraulically Actuated Quadruped robot, Rathod and collaborators achieved the

ability to maintain the intended user speed while adjusting to omnidirectional walking on level terrain. Furthermore, they demonstrated the robot's capability to move across a stationary pallet and adjust to a relocated pallet while locomotion, effectively mitigating external disturbances (Rathod, 2021). Whole-body Control (WBC) approaches have demonstrated significant advancements in controlling legged motion (Farshidian F. a., 2017; Fahmi S. a., 2019). Their primary characteristic lies in employing optimization methods to address motion control challenges. WBC enables the accomplishment of multiple tasks optimally by utilizing the entire dynamics of the robot and considering both actuation limitations and contact interactions. These tasks encompass maintaining balance, interacting with the environment, and executing dynamic motion across diverse terrains (Fahmi S. a., 2019). These duties are performed at the end effectors of the robot but can also involve interactions anywhere on the robot's limb (Henze B. a., 2017), or even facilitate cooperative manipulation tasks between multiple robots (Bouyarmane, 2018). The experimental findings demonstrate the potential for highly dynamic and agile gaits on the ANYmal (Bellicoso C. D., 2017) quadruped robot, which utilizes torque-controllable actuators with series elastic elements. This achievement is facilitated through the integration of a motion planning system founded on a hierarchical whole-body controller and a streamlined dynamic model. The concept of zero moment inertia (ZMP) has been extensively explored in the literature on bipedal walking. It refers to the location situated on the horizontal surface where the resultant moment arising from gravitational and inertial forces is exerted. aligns with the surface normal, indicating that the robot is not tipping (Sardain, 2004). Dynamic balance is attained when contact forces counteract gravitational and inertial forces directly. Thus, the ZMP criterion stipulates that stable dynamic walking is assured while the Zero Moment Point is contained within the geometric area delineated by the contact of the foot and the surface of the ground (Liu F. a., 2010). The motion planning mechanism, rooted in the stability criterion of the ZMP, iteratively adjusts the designated path considering both the present walking pattern and the status of the robot. Meanwhile, the whole-body controller strives to conform to the predetermined plan by resolving a hierarchical structure of objectives. The quasi-direct drive (QDD) method, devoid of an elastic component (Seok S. a., 2012; Bosworth, 2015), due to its low gear ratio, demonstrates a high level of backdrivability and possesses a wide torque control bandwidth, facilitating the emulation of user-defined nonlinear stiffness and damping

characteristics that surpass conventional capabilities of Series Elastic Actuators (SEAs). The MIT Cheetah series and ALPHRED are successful medium-sized quadrupeds, demonstrating the exceptional maneuverability exhibited is akin to that observed in quadrupedal robots powered by hydraulic systems, as well as outstanding capability in traversing uneven terrain and navigating stairs solely relying on proprioceptive feedback (Park, 2017; Hooks, 2020). Small-sized dynamic quadrupeds such as Unitree A1 and Jueying Mini (Sombolestan, 2021; Kim J. a.-J., 2021) represent recent advancements in the utilization of modular QDD actuators. PADWQ is constructed entirely from readily available components and standard 3D printers, representing a recent advancement that facilitates the creation and sharing of intricate 3D parts without the need for expensive CNC machining or casting processes. Unlike robots like Charlotte, RealAnt, and Lilibot, which rely on position-controlled servo motors, limiting their dimensions, performance, and the execution of matered control methods, PADWQ utilizes Gyems RMD-X8 and RMD-X8 Pro series actuators. Overall, both Gyems actuators offer promising performance compared to the Mini Cheetah actuator, particularly given that their market prices are marginally above the cost of materials (BOM) for the Mini Cheetah actuator (Garc{\'\i}a-C{\'a}rdenas, 2020; Boney, 2020; Sun, 2020; Kim J. a.-J., 2021). Joonyoung et al. designed a three-degree-of-freedom leg for PADWQ, utilizing a knee actuation mechanism employing a four-bar parallelogram linkage. and exploiting the standard 3D printing manufacturing process. Their research indicates that the leg components can endure approximately 6.5 times the body weight before failure, which is only slightly less than the values for the Mini Cheetah, even though being composed of plastic material. The leg parts produced through 3D printing exhibit a lower level of rigidity compared to their metal counterparts. This could probably pose a problem when the robot is executing slower and meticulous movements, or when it possesses extended limb proportions (Kim J. a.-J., 2021). Several methods have been employed to activate the knee joint using a remote actuator. SLP or ASLP leg design includes linkage (Spr{\"o}witz, 2013), timing belt (Ramos, 2018), and roller chain (Bledt G. a., 2018). Knee designs driven by timing belts and roller chains contain two primary profits over linkage designs. Firstly, further gear reduction can be readily incorporated through the utilization of pulleys or gears with varying sizes. Secondly, the knee joint's movement range remains unaffected by the linkage, allowing for unrestricted motion (Kim J. a.-J., 2021). Animals demonstrate remarkable agility as they navigate complex terrains,

displaying a variety range of acrobatic and agile skills. The exploration of control methodologies for legged locomotion has been a longstanding pursuit in robotics, with extensive investigations proposing various strategies for controlling legged systems (Miura, 1984; Raibert M. H., Hopping in legged systems—modeling and simulation for the two-dimensional one-legged case, 1984; Goswami, 1999; Geyer, 2003; Yin, 2007; Coros S. a., Generalized biped walking control, 2010; Bledt G. a., 2018). However, formulating such control strategies typically entails an extended developmental period and requires significant expertise in both the fundamental system and the intended behaviors. Despite significant advancements in this regard, the abilities earned by these systems yet do not correspond to the fluidity and elegance of the motions observed in the animal world. Many current methodologies require extensive expertise and manual labor to design each behavior, constraining the resulting capabilities to the designer's comprehension of dynamic and fast behaviors. While trajectory optimization and model predictive control offer potential solutions to reduce manual efforts in the design process, the complex and high-dimensional dynamics of legged systems often demand simplified models to create manageable optimization problems (De Lasa, 2010; Gehring, 2016; Di Carlo, 2018; Apgar, 2018). However, these simplified models tend to be tailored to special tasks and need a substantial understanding of each skill's properties. Motion imitation gives a comprehensive method for robots to execute diverse behaviors that would be challenging with manual programming into control systems (Pollard, 2002; Grimes, 2006; Suleiman, 2008; Yamane, 2010). Yet, the application of motion imitation in legged robots has mainly focused on behaviors emphasizing upper-body movements, with relatively static lower-body motions, where equilibrium control is separately achievable (Nakaoka, 2003; Kim S. a., 2009; Koenemann, 2014). In contrast, agents in simulation environments have replicated significantly more dynamic skills (Muico, 2009; Lee Y. a., 2010; Coros S. a., 2011; Liu L. a., 2016). Recently, integrating motion mimicry with reinforcement learning has effectively entered a wide range of significant acrobatic possibilities in simulation settings (Peng X. B., 2018; Peng X. B., 2018; Lee S. a., 2019). However, the intricacy of reinforcement learning methodologies and the limitations imposed by physical factors have hindered the replication of many simulated capabilities in real-world scenarios. Learning-based approaches offer promise in enhancing the agility of legged robots and reducing manual labor in controller development. Particularly, reinforcement learning (RL)

emerges as a powerful and versatile method for crafting controllers capable of executing complex skills (Coros S. a., Robust task-based control policies for physics-based characters, 2009; Peng X. B., 2016; Heess, 2017; Peng X. B., 2018; Liu L. a., 2018). Despite promising outcomes in simulations, RL-trained agents often exhibit unnatural behaviors that may pose risks or prove impractical in real-world deployment. Additionally, designing reward functions to induce desired behaviors can require meticulous and task-specific tuning. The difficulties of using RL in actual scenarios have led to the adoption of domain transfer methods, where strategies are trained within simulated settings (source domain) and then transferred to actual settings (target domain). The process of transferring simulations to real-world scenarios can be improved by refining the precision of simulations (Tan J. a., 2018; Xie, 2020) or by enriching simulators with real-world data (Tan J. a., 2016; Hanna, 2017; Hwangbo, 2019; Lowrey, 2018; Chebotar, 2019). However, creating highly accurate simulators remains a challenging task, as even advanced simulators only provide a fundamental estimation of the complex dynamics observed in actual environments. To overcome this challenge, methods like domain randomization can be integrated into the training regimen to enhance policy adaptability to dynamic changes (Sadeghi, 2016; Tobin, 2017; Pinto, 2017; Peng X. B., 2018; Andrychowicz, 2020). Furthermore, sample-efficient adaptation methods like fine-tuning (Rusu, 2017) and meta-learning (Duan, 2016; Finn, 2017; Nagabandi, 2018) can be utilized to enhance the efficiency of pre-trained strategies during transitions to new domains. RL has proven fruitful in autonomously learning motion abilities both in simulated environments (Peng X. B., 2018; Liu L. a., 2018; Lee S. a., 2019) and real-world scenarios (Kohl, 2004; Tedrake R. a., 2004; Endo, 2005; Tan J. a., 2018; Haarnoja, 2018; Hwangbo, 2019). These systems train strategies utilizing manually designed reward functions tailored to every special ability, a process that can be challenging, especially for much more sophisticated treatment. To address these challenges, Peng et al. devised an automated method to develop controllers capable of executing various behaviors for legged robots. This approach relies on reference motion data and integrates multiple learning-based techniques into a unified framework. By incorporating efficient domain adaptation strategies during training, the system learns adaptable policies in simulation, facilitating their seamless transfer for deployment in real-world scenarios. The process involves three key steps: motion retargeting, motion mimics, and domain adjustment, which collectively enable the synthesis of effective control policies (Peng

X. B.-W., 2020). The domain of legged robotics, drawing inspiration from natural systems, seeks to develop autonomous platforms capable of navigating rugged and intricate environments. Notably, while the DARPA subterranean challenge, quadruped robots saw widespread adoption and achieved notable success (Tranzatto, 2022; Bouman, 2020). However, traversing sophisticated grounds that demand accurate step positioning, such as adverse obstacles and stepping stones continues to pose significant challenges. A fundamental hurdle arises from the interplay between terrain characteristics and system dynamics, which puts limits on contact position, force application, and timing. While established methods exist for model-based locomotion, including perceptive approaches for slow, static gaits (Kalakrishnan, 2010; Griffin, 2019) and blind locomotion on flat surfaces (Bellicoso C. D., 2018; Di Carlo, 2018), adapting these techniques to address complex terrains remains a formidable task. Recent advancements in learning-based controllers have demonstrated remarkable progress in extending blind locomotion capabilities to challenging terrains with exceptional robustness (Lee J. a., 2020; Miki, 2022). Nevertheless, the seamless integration of perception for achieving synchronized and accurate positioning of the feet remains an ongoing area of in-process investigation. Several strategies have been proposed to enhance dynamic locomotion across rough terrain by integrating perceptual data into foothold selection algorithms (Jenelten F. a., 2020; Villarreal, 2020). These methods typically follow a hierarchical structure, initially prioritizing the selection of footholds before improving torso movement. While this breakdown decreases the computational intricacy, it necessitates manual coordination between the two modules. Furthermore, the separation of leg movements from torso optimization complicates the consideration of kinematic constraints and collision prevention between limbs and the ground. Trajectory optimization techniques, which involve the joint optimization of torso and leg movements, have demonstrated remarkable efficacy in simulation settings (Mordatch, 2012; Dai, 2014) and eliminate the requirement for manually engineered coordination between the torso and feet. By incorporating the entire terrain into the optimization process, these methods can automatically discover complex motions. However, the computational demands often exceed practical limits for real-time deployment. Moreover, the non-convexity, non-linearity, and discontinuity resulting from optimizing across various types of lands are able to lead to convergence issues and suboptimal solutions. Addressing these challenges requires dedicated efforts to provide reliable initial guesses for feasible motions (Melon, 2020).

When adopting a quasi-static gait pattern with a predetermined sequence of steps, the planning complexities associated with rugged terrain can be simplified by deconstructing them into separate touch transitions., as evidenced by the research on LittleDog (Kalakrishnan, 2010; Kolter, 2008). By considering the next foothold in a one-step-ahead manner, one can assess its kinematic feasibility, its compatibility with the terrain, and the likelihood of achieving a transition that is statically stable. This issue can be effectively addressed by examining and assessing potential footholds through sampling (Tonneau, 2018). Subsequently, a trajectory free of collision for the swinging leg toward the desired foothold can be computed according to a Signed Distance Function (SDF), for instance, using the CHOMP algorithm (Zucker, 2013). Fankhauser et al. (Fankhauser, 2018) successfully achieved complete onboard realization and control with such a method. Alternatively, rather than employing planning with a one-step foresight, an RRT graph can be constructed to plan further into the future (Belter, 2016). Achieving similar outcomes is possible by sampling over templated foothold transitions (Mastalli C. a., 2020; Mastalli C. a., 2015). Several strategies originally designed for flat terrain, where footholds are specified before optimizing the movement of the torso, have been adapted for traversing rough terrain (Bajracharya, 2013; Bazeille, 2014). These approaches typically utilize Raibert heuristics (Raibert M. H., Legged robots that balance, 1986) to choose the subsequent foothold and adjust it according to perceptual data, such as traversability estimates (Wermelinger, 2016). Building upon the study of Bellicoso et al. (Bellicoso C. D., 2018), further advancements include batch searches for possible footprints according to provided terrain maps and footprint scoring (Jenelten F. a., 2020). Similarly, Kim et al. (Kim D. a., 2020) presented a foot position that is adjusted based on visual data, leading to agile trotting and leaping movements. Another proposal (Magana, 2019) introduces a convolutional neural network (CNN) trained to expedite the online valuation of such footprint adjustment pipelines. This CNN is integrated with the MPC policy presented (Di Carlo, 2018) to attain sensory-based movement in a simulated environment (Villarreal, 2020). Alternatively, in (Gangapurwala, 2022) and (Yu, 2021), an RL policy replaces heuristic footprint selection. However, because footprint positions are determined before optimizing torso movement, their impact on dynamic balance and the practicality of movement aren't explicitly addressed, necessitating extra rules to synchronize the movements of the feet and torso to adhere to whole-body dynamics and kinematics. Furthermore, considering leg collisions with the terrain

becomes challenging once the foothold is fixed. Recently, there has been a shift towards using Kinodynamic (Farshidian F. a., 2017), Centroidal (Orin, 2013; Meduri, 2023), and full dynamics models (Pardo, 2017; Mastalli C. a., 2022) To concurrently optimize the positions of feet in three dimensions and body movements. On the other hand, enhancing single rigid body dynamics (SRBD) models or other simplified torso models with decision variables for Cartesian footprint locations (Winkler, 2018; Jenelten F. a., 2022). Real-time feasible approaches have been suggested (Bledt G. a., 2017), velocity (Farshidian F. a., 2017), or acceleration level (Neunert, 2018). However, computational complexity increases significantly with higher-dimensional models, particularly in locomotion on flat terrain. Lastly, various methods upgrade gait timings or also the touch pattern along with whole-body movement. This is achievable through supplement limits (Mordatch, 2012; Dai, 2014; Posa, 2014), mixed-integer programming (Aceituno-Cabezas, 2017; Marcucci, 2017), or by directly incorporating contact models into the optimization process (Neunert, 2018; Carius, 2018). On the other hand, the period of each touch step can be treated as a decision variable (Winkler, 2018; Ponton, 2018), or determined through bilevel optimization (Farshidian F. a., 2017). Nonetheless, these approaches are prone to be trapped in suboptimal solutions, and effectively solving optimization tasks in real-time remains a persistent challenge.

The utilization of an elevation map holds a significant legacy in legged robotics (Kweon, 1989) and remains a fundamental component in many perceptual locomotion control systems. Strategies employing local exploration or sampling-oriented algorithms can directly interact with this framework for selecting footholds. Even though, integrating terrain into gradient-based optimizations requires further refinement. Winkler et al. (Winkler, 2018) employ an elevation map for both positioning footsteps and avoiding collisions, with foot movement spline limited to initiate and conclude on the terrain through equality limits. An inequality constraint is incorporated to evade terrain during the swing phase. Yet, disregarding terrain discontinuities and non-convexities renders this method susceptible to poor local minima, prompting the development of specialized initialization schemes (Melon, 2020). By Jenelten et al. (Jenelten F. a., 2022), a graduated optimization scheme is adopted, initially optimizing over a smoothed terrain version. Subsequently, the solution from this optimization initializes another over the actual elevation map. Similarly, Mordatch (Mordatch, 2012) broad 3D setting and utilizes a soft-minimum operator to refine the calculation of the nearest point. A constant plan incrementally

heightens the problem's complexity across successive upgrades. Deits et al. (Deits, 2014) delineate a planning approach for navigating challenging terrain grounded on mixed-integer quadratic programming (MIQP). From the terrain, it's possible to derive convex safe areas, and allocating footsteps to these regions is presented as a non-continuous decision. Simplification of the footprint upgrade is achieved by exclusively considering convex, safe areas while scheming. Additionally, the performance necessitated manual seeding of convex areas by a man operative (Griffin, 2019). Grandia et al. (Grandia, 2023) introduced a controller skilled at adaptive and responsive movement in demanding lands. They achieved this by establishing perceptive foot placement constraints via a convex inner approximation of steppable terrain, formulating a nonlinear model predictive control (MPC) problem. Their numerical strategy enables reliable and efficient solution to this problem. Steppability classification, plane segmentation, and a signed distance function (SDF) are precalculated and refreshed at a rate of 20 Hz. Asynchronous precalculation of this data significantly reduces the calculation burden for each MPC repetition, rendering the method real-time able. This method concurrently optimizes foot position, knee collision prevention, and underactuated system dynamics by incorporating the entire joint setup into the model of the system. With this comprehensive information embedded in the upgrade time, the method autonomously discovers intricate movements and demonstrates generalization over diverse terrains and gaits necessitating accurate foot position and comprehensive body synchronization.

# 3. QUADRUPED ROBOT MODEL

Although numerous valuable studies have been conducted on the optimization of legged robots, to the best of our knowledge, no studies are addressing the behavior of legged robots during scaling. Understanding the variations in mechanical parameters such as joint torques, power consumption, MCOT (Mechanical Cost of Transport), and reaction forces during scaling can facilitate effective and advanced optimization of legged robots. In this study, we analyze a standard Unitree A1 quadruped robot at various sizes to elucidate the changing behaviors of mechanical parameters that influence the dynamics of the robot.

## 3.1 Unitree A1 Model

The Unitree A1, an advanced quadruped robot utilizing QDDs (Sombolestan, 2021), serves as our standard model for scaling. Owing to its structural characteristics, this robot offers a suitable framework for capturing valuable data applicable to various types of legged robots, including series elastic and QDDs. The Unitree A1 offers a more budget-friendly option compared to other premium quadruped robots like Boston Dynamics' Spot, making it available to a broader range of users and applications. Its lightweight and fast speed enable it to execute swift and agile movements, which is beneficial in dynamic settings. However, despite its agility, the A1 may struggle with rough or uneven terrain compared to more robust models like the Boston Dynamics Spot, which are specifically built for challenging environments (Katz, H.,2021).

**Figure 3.1:** Unitree A1 robot (https://www.prosmt-market.com/marka/unitree)

## 3.2 Designed Quadruped Robot Model

As dimensional drawings of the Unitree A1 quadruped robot were unavailable, we undertook the task of redesigning and assembling its components, aiming to approximate the dimensions of the existing Unitree A1 model available in the market. Figure 3.2 illustrates the reference model. In this study, we assume the robots walk at a constant speed on even flat terrain. The effect of fluid mechanics, such as air resistance while walking, is not considered, and the robot is assumed to lack backdrivable ability. Ground acceleration and reaction forces between the end effectors and terrain are accounted for. The thesis explores the behavior of mechanical principles affecting the robot without regard to the type of motors, motor placement architecture, and the presence or absence of any elastic elements. This simplified model enables us to provide the necessary foundational and fundamental data applicable to different types of legged robots. By understanding the behavior of a robot during scaling and knowing the required mechanical parameters, such as hip torque, designers can determine the appropriate actuator type and placement or incorporate elastic elements.

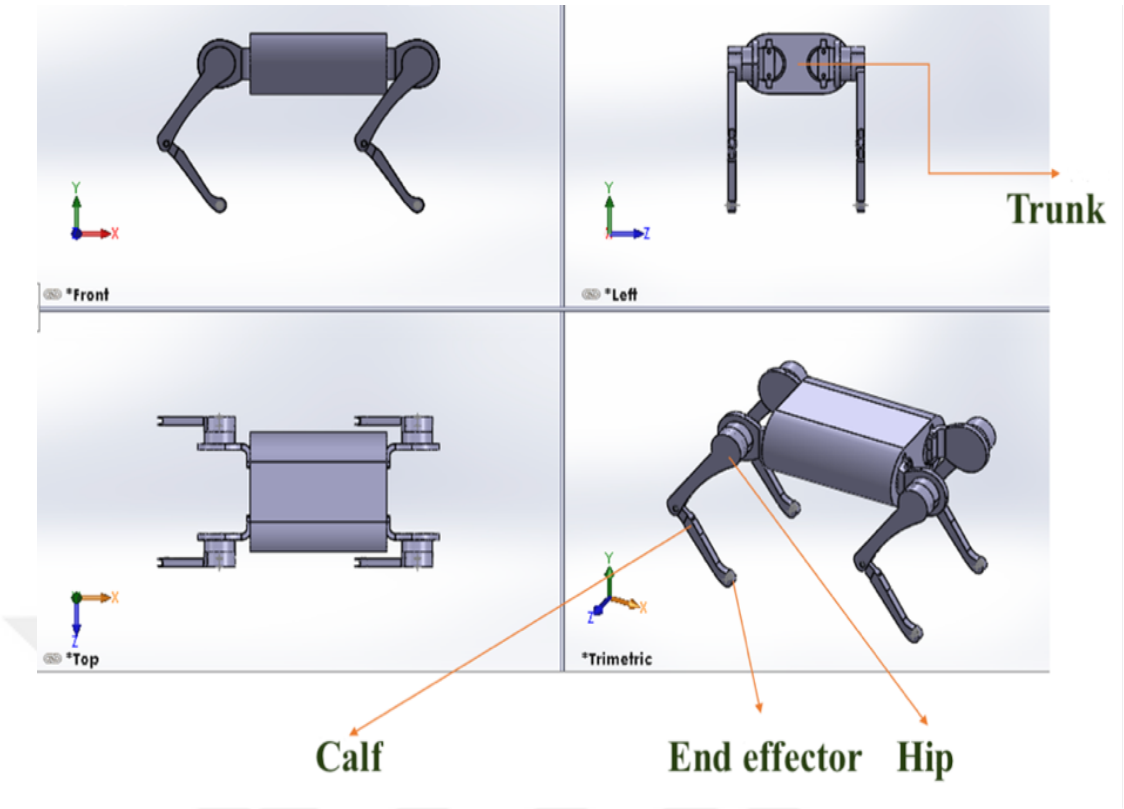


**Figure 3.2:** The reference model is based on the Unitree A1 quadruped robot.

### 3.3 Scaling Idea

Using CATIA V5 R21, we designed and assembled the robot's different parts such as the Torso, Hips, and Calves. With the aim of the SolidWorks motion analysis environment, the robot is scaled and simulated through five different scenarios. In all scenarios, the robots walk on even flat terrain at a constant speed, but in all scenarios, the starting position remains the same as shown in Figure 3.3. Simulations last for five seconds. At the start of the simulation, the robots are dropped from a close distance onto the terrain. Generally, during the initial 0.8 seconds of the simulations, we observe the adjustment phase. The trajectory of the end effector is depicted in Figure 3.4. Table 3.1 presents the robots' dimensions, mass, material, walking speed, and the length and height of each step of the end effector. In the first scenario, from the reference robot (robot one) to the fourth robot, there is a 0.3 increase in the length of the Torso, arms, and Calves.

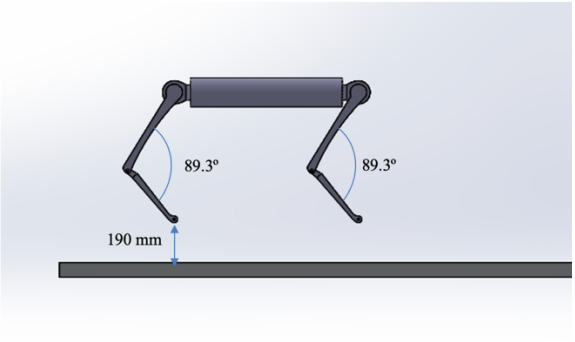


**Figure 3.3: Starting position in all robots.**

The second scenario involves an increase in the length of the step size. In the third scenario, the step length from the second scenario is maintained, but there is an increase in the step height, analogous to the second scenario.

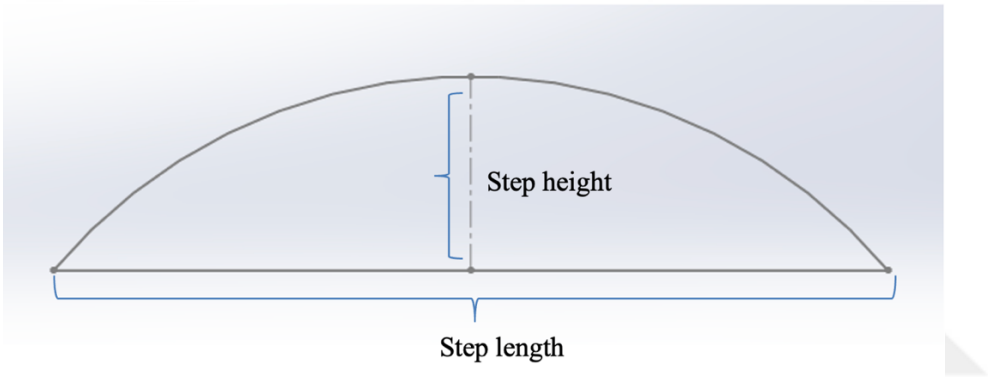


**Figure 3.4: The trajectory of the end effector.**

In the fourth scenario, the step dimensions from the second scenario are retained, but the length of the Torso remains constant while there is a 0.3 increase in the length of the arms and calves.

**Table 3.1:** Scaled robots' general data.

| Scenari | Robot | Arm length (mm) | Calf length (mm) | Torso length (mm) | Torso width (mm) | Torso heigth (mm) | Total mass (kg) | Material | Step length (mm) | Step height (mm) | Linear speed mm/s |
|---|---|---|---|---|---|---|---|---|---|---|---|
| 1, 2, 3 | 1 | 160 | 140 | 250 | 200 | 100 | 15.3 | 2018 Alloy | 120 | 27 | 250 |
| | | | | | | | | | 165 | 27 | |
| | | | | | | | | | 165 | 40 | |
| | 2 | 208 | 182 | 325 | 200 | 100 | 18.7 | 2018 | 120 | 27 | 250 |

| | | | | | | | | | | | |
|---|---|---|---|---|---|---|---|---|---|---|---|
| | | | | | | | | Alloy | 165 | 27 | |
| | | | | | | | | | 165 | 40 | |
| | 3 | 256 | 224 | 400 | 200 | 100 | 22.6 | 2018 Alloy | 120 | 27 | 250 |
| | | | | | | | | | 165 | 27 | |
| | | | | | | | | | 165 | 40 | |
| | 4 | 304 | 266 | 475 | 200 | 100 | 28.7 | 2018 Alloy | 120 | 27 | 250 |
| | | | | | | | | | 165 | 27 | |
| | | | | | | | | | 165 | 40 | |
| 4, 5 | 1 | 160 | 140 | 475 | 200 | 100 | 28 | 2018 Alloy | 165 | 27 | 250 |
| | | 256 | 224 | 250 | 200 | 100 | 15.76 | | | | |
| | 2 | 208 | 182 | 475 | 200 | 100 | 28.13 | 2018 Alloy | 165 | 27 | 250 |
| | | 256 | 224 | 325 | 200 | 100 | 19 | | | | |
| | 3 | 256 | 224 | 475 | 200 | 100 | 28.43 | 2018 Alloy | 165 | 27 | 250 |
| | | 256 | 224 | 400 | 200 | 100 | 22.62 | | | | |
| | 4 | 304 | 266 | 475 | 200 | 100 | 28.73 | 2018 Alloy | 165 | 27 | 250 |
| | | 256 | 224 | 475 | 200 | 100 | 28.44 | | | | |

**Table 3.1(continued):** Scaled robots' general data.

# 4. SIMULATION STUDIES

We utilized eight motors positioned at the center of mass of each joint: four motors in the hips and four motors in the knees. We divided the trajectory, as depicted in Figure 3.3, into eight points and subsequently measured the positions of the arms and calves. All hip motors follow different displacement patterns to achieve the desired constant linear speed for all scenarios and robots. In essence, the angular displacement and angular speed across all scenarios and robots vary. The corresponding plots are presented in the following sections.

## 4.1 General Hypothesis

The study aims to analyze the impact of varying robot dimensions and operational parameters on performance metrics, such as torque requirements, contact forces, and cost of transport. By systematically altering robot sizes, and step parameters, and comparing them with existing robots in the literature, the research seeks to identify optimal configurations for efficient robotic locomotion. The analysis includes four different sizes of robots, each subsequent iteration expanding the robot size by 30%, comparing specified metrics for constant linear velocity, step height/body height ratio, and step length/body length ratio. Additionally, one robot is selected to compare constant linear velocities with constant step length and step height, different step lengths with constant step height and linear velocity, and different step heights with constant step length and linear velocity. Further comparisons involve scaling the leg sizes of one robot while keeping the body constant, and scaling the body length and width while keeping the legs constant, each at four different levels, to assess the impact on torque requirement, contact forces, and cost of transport. Finally, the cost of transport of these simulations is compared with other state-of-the-art robots in the literature to evaluate their efficiencies.

### 4.2 Common Aspects of Scenarios

In all scenarios, different scaled form of the designed QR model is employed with constant linear speed while walking on flat terrain to eliminate the effect of speed on energy consumption. Trot walking gait type was used in the analysis and simulations. All the robots use the same material and experience vertical gravitational acceleration to the body. Table 3.1 provides detailed specifications for various robot models simulated in this study, highlighting their dimensions, material, and performance characteristics. detailing their physical dimensions, material, and performance attributes. In scenarios one, two, and three, robot 1 has an arm length of 160 mm, a calf-length of 140 mm, a torso length of 250 mm, a torso width of 200 mm, a torso height of 100 mm, and a total mass of 15.3 kg. Robot 2 features an arm length of 208 mm, a calf-length of 182 mm, a torso length of 325 mm, a torso width of 200 mm, a torso height of 100 mm, and a total mass of 18.7 kg. Robot 3 is characterized by an arm length of 256 mm, a calf length of 224 mm, a torso length of 400 mm, a torso width of 200 mm, a torso height of 100 mm, and a total mass of 22.6 kg. Robot 4 includes an arm length of 304 mm, a calf length of 266 mm, a torso length of 475 mm, a torso width of 200 mm, a torso height of 100 mm, and a total mass of 28.7 kg. The step length is 120 mm, 165 mm, and 165 mm in scenarios one, two, and three, respectively, while the step height is 27 mm, 27 mm, and 40 mm. In scenarios four and five the step length is 165 mm, and the step height is 27 mm. In scenario four, Robot 1 has an arm length of 160 mm, a calf length of 140 mm, a torso length of 475 mm, a torso width of 200 mm, a torso height of 100 mm, and a total mass of 28 kg. Robot 2 in this set has an arm length of 208 mm, a calf length of 182 mm, a torso length of 475 mm, a torso width of 200 mm, a torso height of 100 mm, and a total mass of 28.13 kg. Robot 3 features an arm length of 256 mm, a calf length of 224 mm, a torso length of 475 mm, a torso width of 200 mm, a torso height of 100 mm, and a total mass of 28.43 kg. Lastly, Robot 4 in this set has an arm length of 304 mm, a calf length of 266 mm, a torso length of 475 mm, a torso width of 200 mm, a torso height of 100 mm, and a total mass of 28.73 kg. In scenario five, Robot 1 has an arm length of 256 mm, a calf length of 224 mm, a torso length of 250 mm, a torso width of 200 mm, a torso height of 100 mm, and a total mass of 15.76 kg. Robot 2 in this set has an arm length of 256 mm, a calf length of 224 mm, a torso length of 325 mm, a torso width of 200 mm, a torso height of 100 mm, and a total mass of 19 kg. Robot 3 features an arm length of

256 mm, a calf length of 224 mm, a torso length of 400 mm, a torso width of 200 mm, a torso height of 100 mm, and a total mass of 22.62 kg. Lastly, Robot 4 in this set has an arm length of 256 mm, a calf length of 224 mm, a torso length of 475 mm, a torso width of 200 mm, a torso height of 100 mm, and a total mass of 28.44 kg. All robots are made of alloy, and have a linear speed of 250 mm/s.

In this study, in the first scenario, we define the length and height of the trajectory as 120 mm and 27 mm, respectively. The length of the arms, torso, and legs increases in the four robots to observe the effect of scaling. The length increase follows the same pattern in scenarios one to three with a 30% coefficient. In the second scenario, we increased the length of the trajectory from 120 mm to 165 mm to observe the effect of length increase in trajectory. Then in the third scenario, we defined the length of the trajectory as 165 mm while increasing the height of the trajectory from 27 mm to 40 mm. The fourth scenario maintains the same trajectory length and height as the second scenario, and robot scaling remains consistent except for the Torso. The Torso retains the dimensions of the Torso of the fourth robot in scenario two (the longest). In other words, in this scenario, we scale the robot while keeping the Torso dimension fixed. We compare scenario four with scenario two due to the identical trajectory dimensions. in scenario five, only the Torso is scaled while the arms and legs retain the dimensions of robot three in scenario two. The pattern changes in scenario five compared to the previous scenarios, particularly in scenario two. These different scenarios and scaling patterns lead to a new session in quadruped robot advancement since, to the best of our knowledge, there have not been any studies on quadruped robots' behaviors while scaling. This prepares the fundamental data for an SCA.

## 5. SIMULATION RESULTS

In this section, we compare the results of our simulations on hip torque, calf torque, hip power consumption, calf power consumption, MCOT, and reaction forces between the end effector and terrain. To determine the mentioned parameters.

### 5.1 Scenario One, Two, and Three

All four robots in each scenario exhibit similar patterns of hip torque, calf torque, hip power consumption, calf power consumption, and reaction forces between the end effector and terrain over time, initially displaying minimal torque (close to zero) that gradually increases as time progresses, with fluctuations observed throughout the movement. Despite the increase in robot length by 30% and the changes in the length and height of the trajectory in scenarios one, two, and three, the overall shape and magnitude of the hip torque (Figure 5.1), calf torque (Figure 5.2), hip power consumption (Figure 5.3), calf power consumption (Figure 5.4), and reaction forces (Figure 5.5) remain similar. These changes do not drastically alter the hip torque pattern; instead, they seem to proportionally scale the values up or down. The consistency in the shape of the mentioned mechanical principles curves across different scaled robots and mentioned scenarios suggests that the mentioned probable scenarios and scaling pattern have no significant effect on the scaled robot's dynamics.

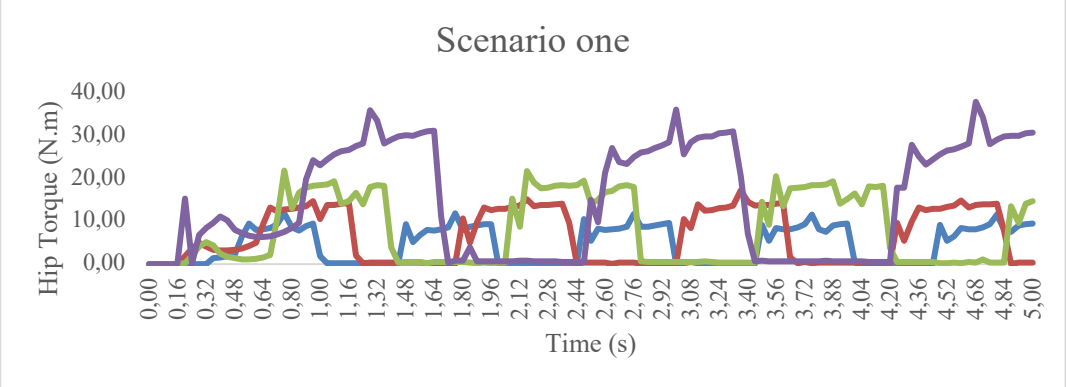


**Figure 5.1:** Similar patterns of hip torque through scenarios 1,2,3.

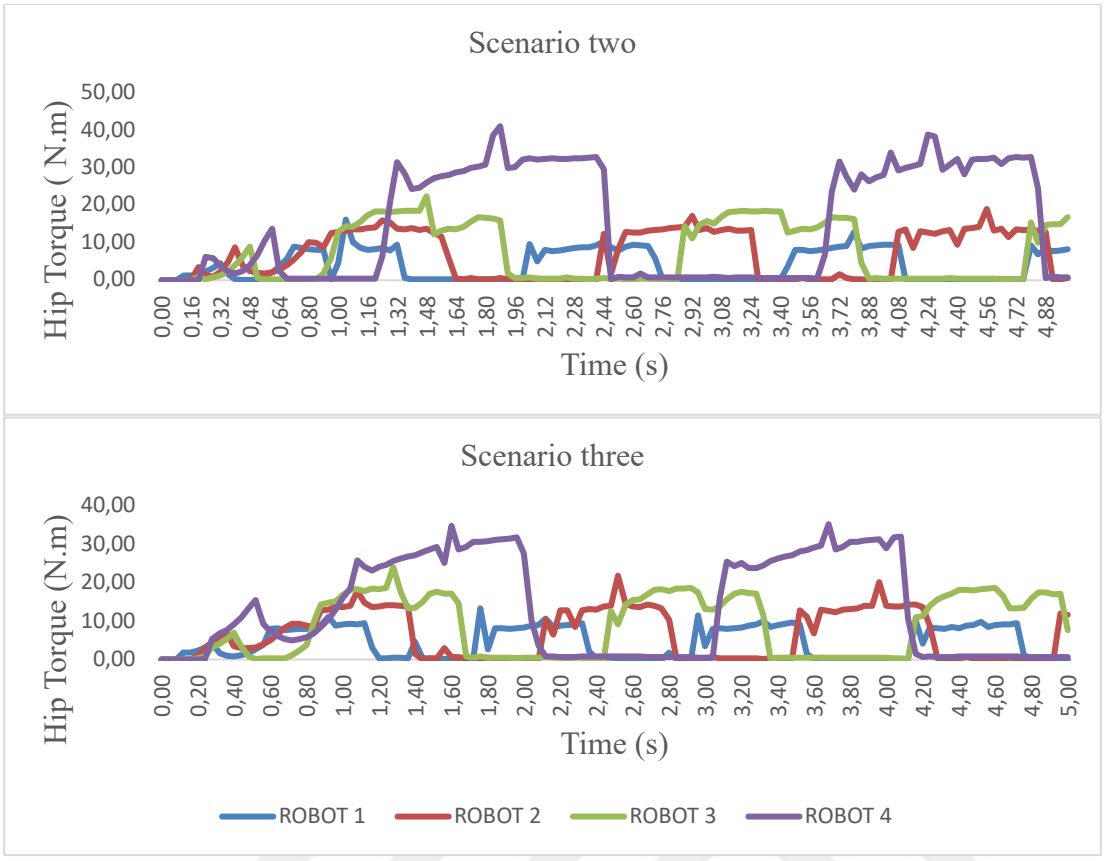


**Figure 5.1(continued):** Similar patterns of hip torque through scenarios 1,2,3.

In each scenario, although the overall pattern is consistent, there are noticeable differences in the magnitude of values between the robots, generally increasing as the robot's length increases.

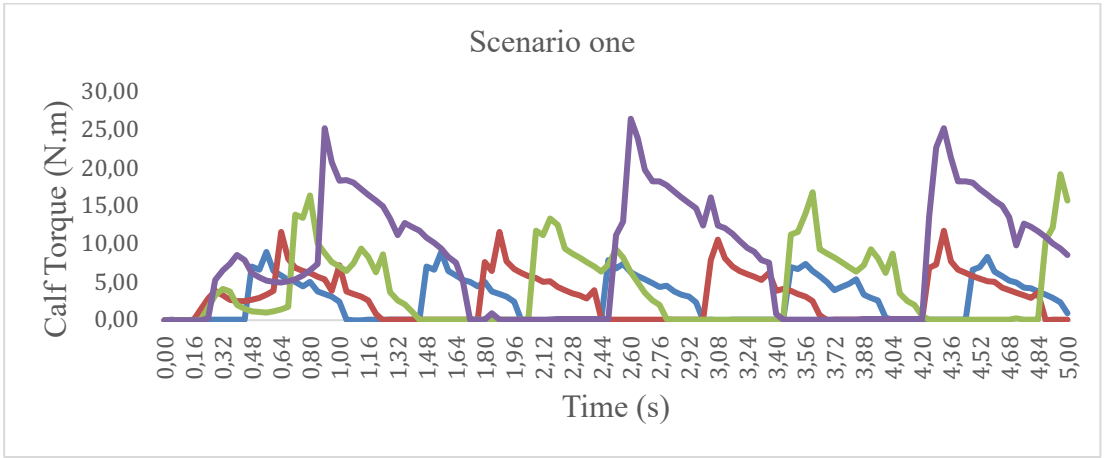


**Figure 5.2:** Similar patterns of calf torque through scenarios 1,2,3.

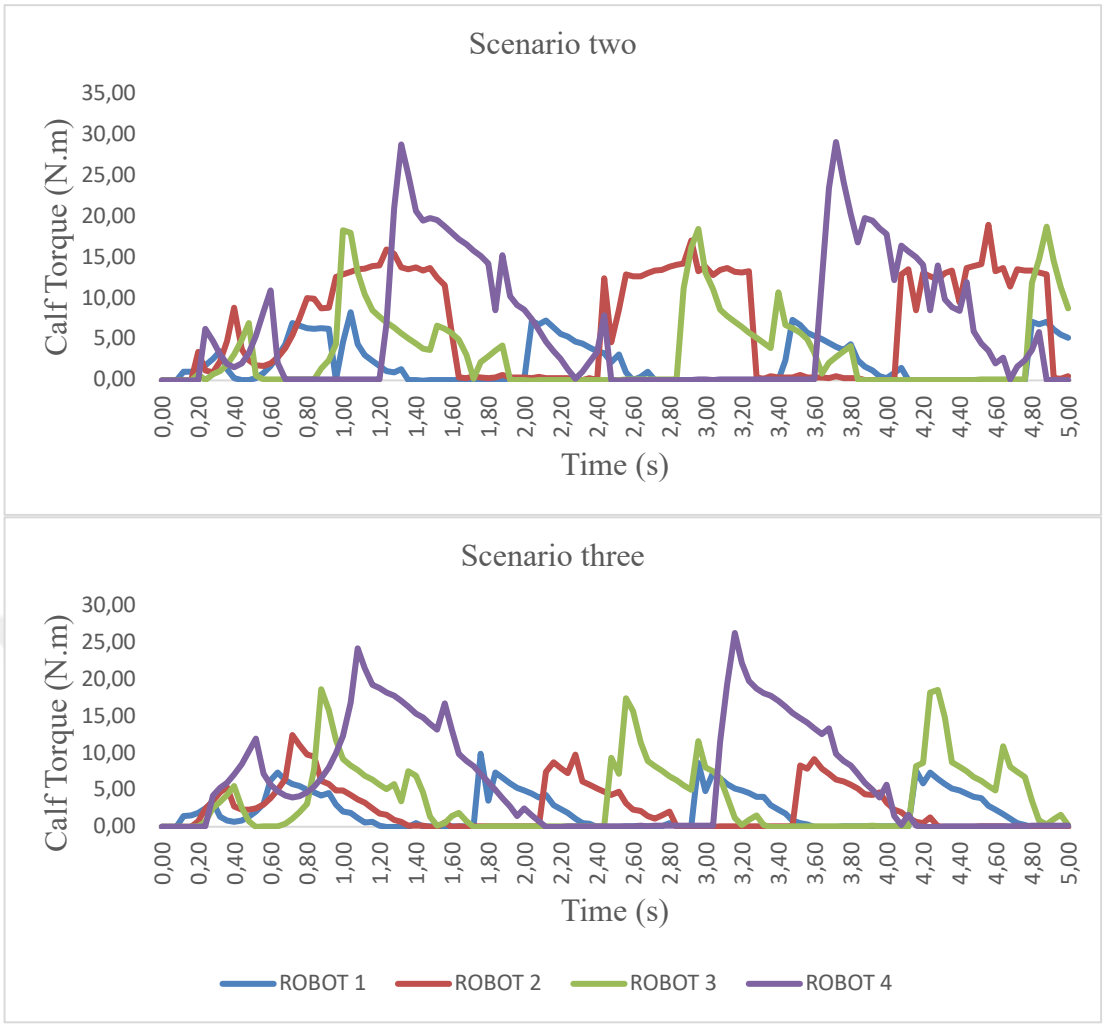


**Figure 5.2(continued):** Similar patterns of calf torque through scenarios 1,2,3.

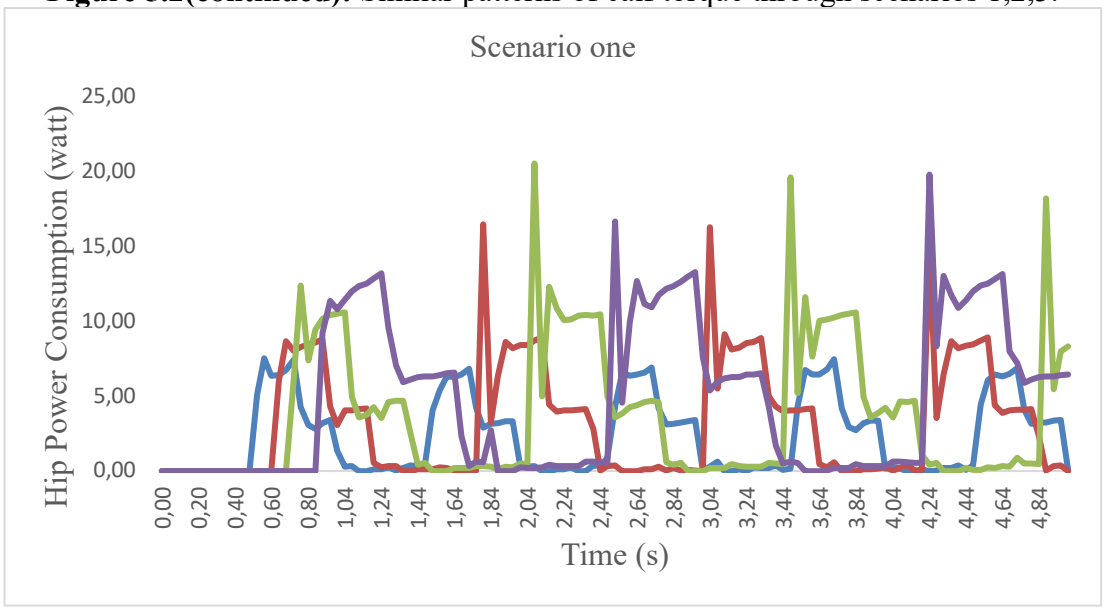


**Figure 5.3:** Similar patterns of hip power consumption through scenarios 1,2,3.

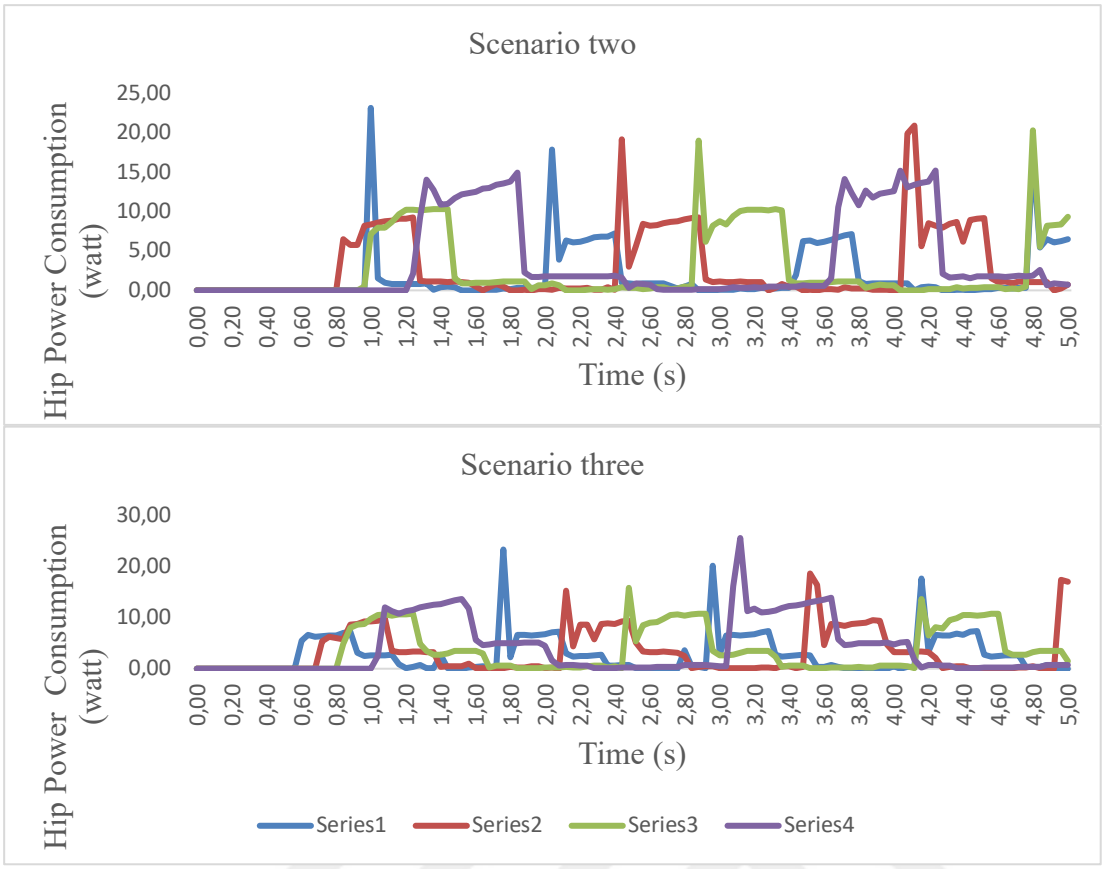


**Figure 5.3( continued):** Similar patterns of hip power consumption through scenarios 1,2,3.

However, this relationship is not strictly linear. There are instances of sudden spikes or drops in values for all robots, indicating transient events or adjustments in the walking motion, which might correspond to specific phases of the walking cycle.

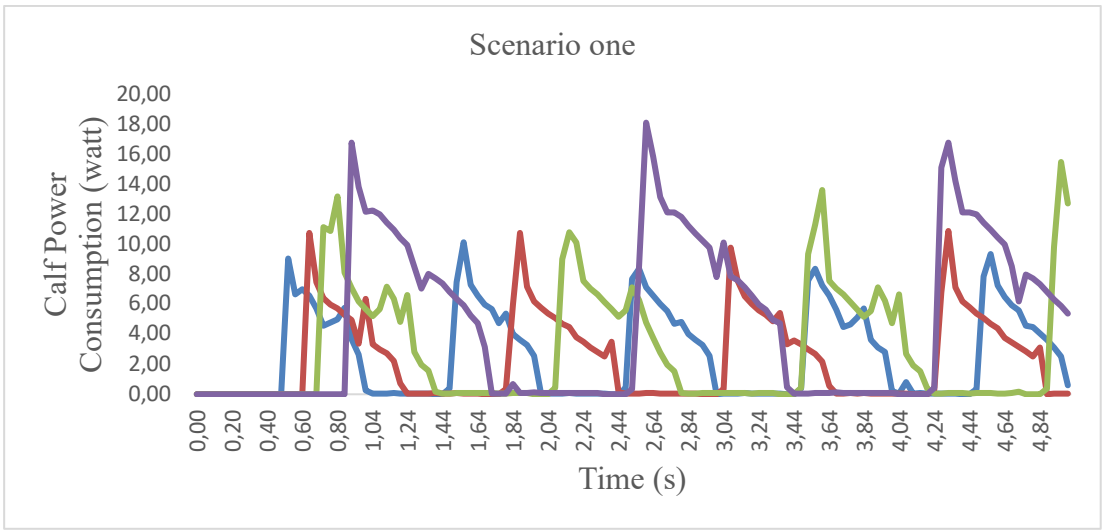


**Figure 5.4:** Similar patterns of hip power consumption through scenarios 1,2,3.

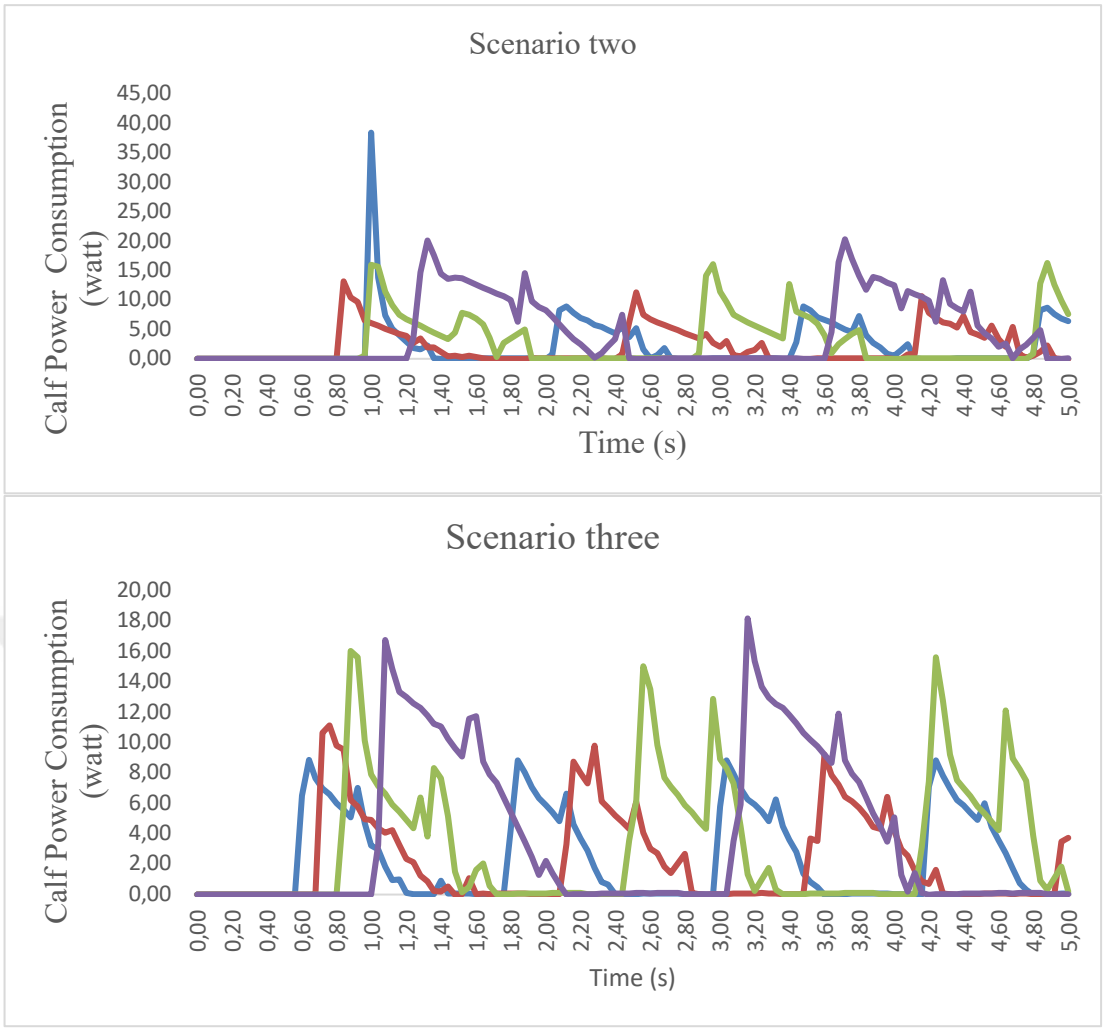


**Figure 5.4(continued):** Similar patterns of hip power consumption through scenarios 1,2,3.

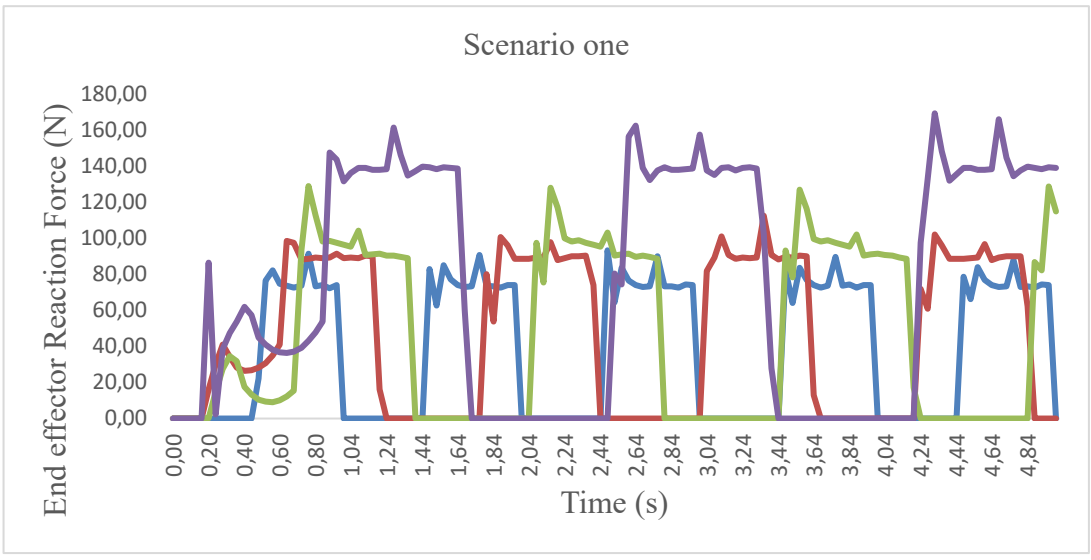


**Figure 5.5:** Similar patterns of end effector reaction forces through scenarios 1,2,3.

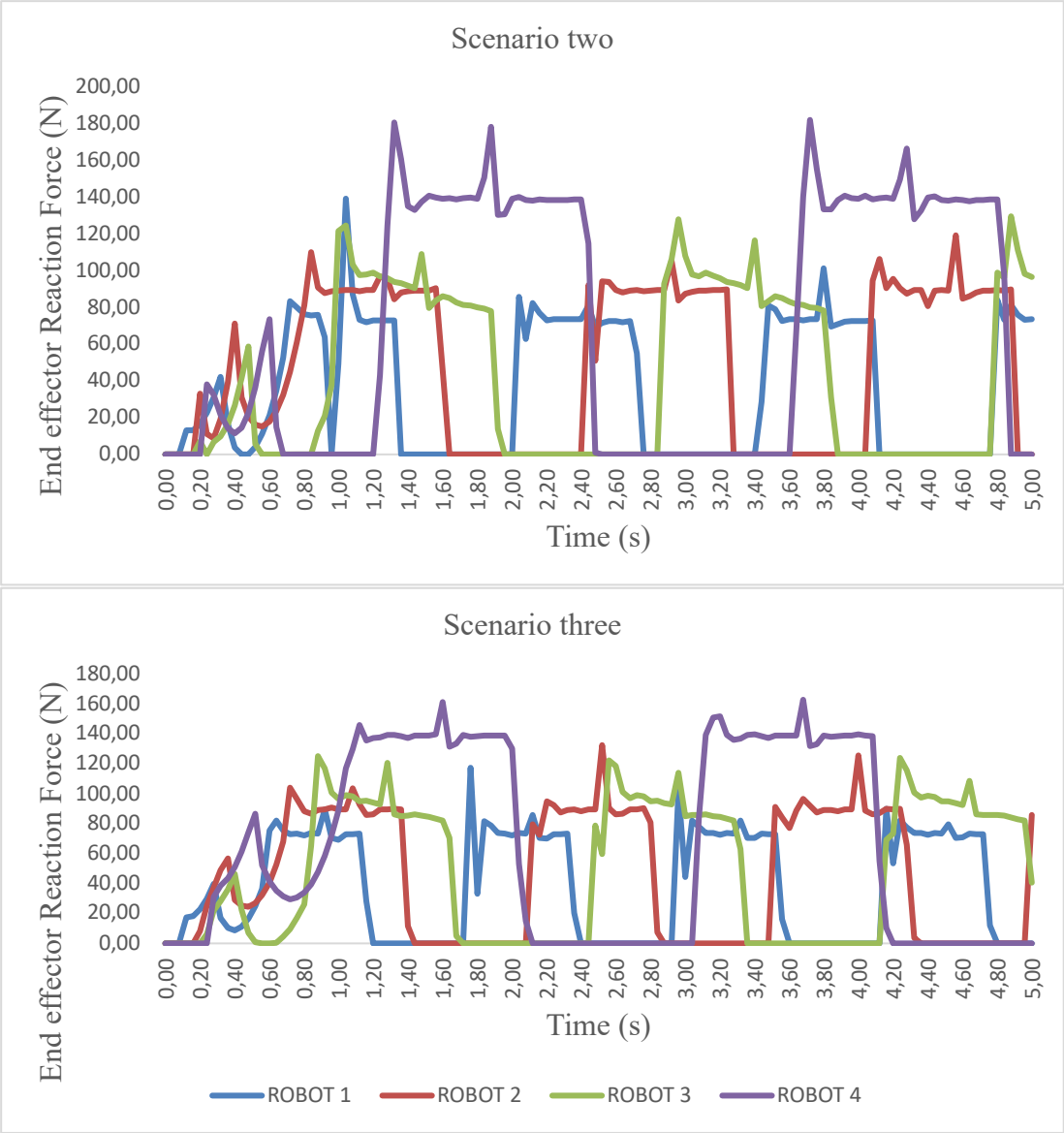


**Figure 5.5(continued):** Similar patterns of end effector reaction forces through scenarios 1,2,3.

On the other hand, the magnitude of the values for the corresponding robots approximately remains the same. The only difference is in the angular displacement of the motors. As an example, the angular displacement of robot three through scenarios one, two, and three are shown in Figure 5.6.

In other words, if the motors have adjustable capabilities in terms of motor angular speed and possess logical power and torque, the robot can be scaled using the aforementioned scaling patterns and scenarios.

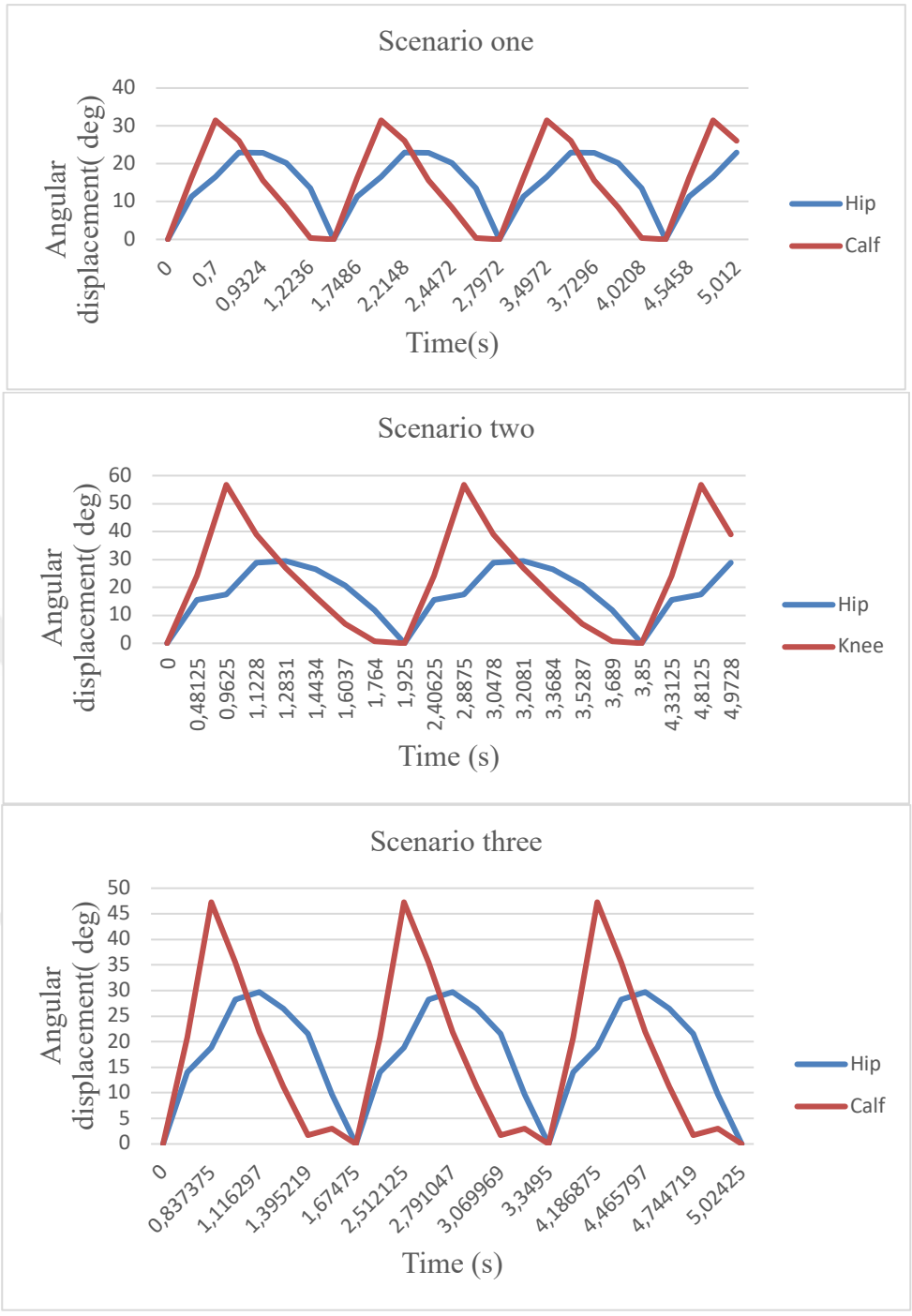


**Figure 5.6:** The angular displacement of robot 3 through scenario 1,2,3.

### 5.2 Scenarios Four and Five

We compare scenario four with scenario two due to the identical trajectory dimensions. Upon comparison, we observed that the pattern and approximate magnitude of the hip torque (Figure 5.7), calf torque (Figure 5.8), hip power (Figure 5.9), and calf power (Figure 5.10) remain consistent, albeit with a slight increase in the mentioned parameters for robots one, two, and three due to the enlarged Torso size.

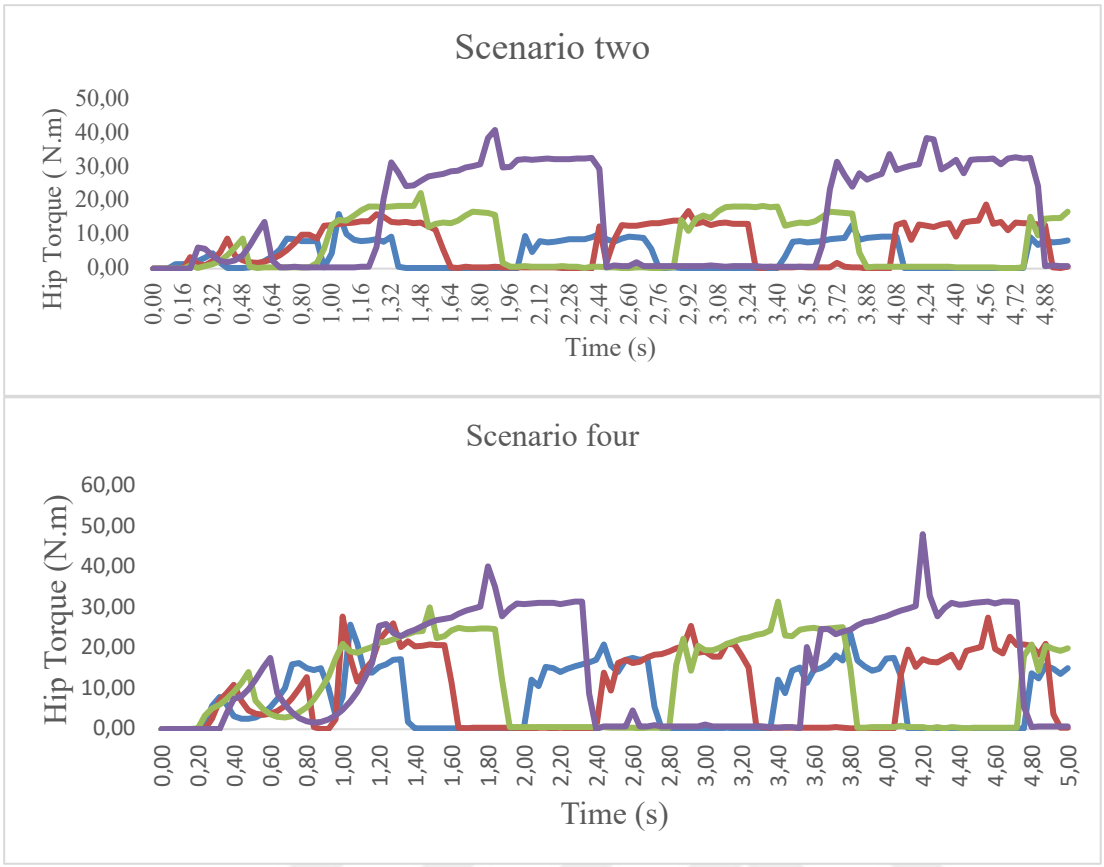


**Figure 5.7:** Similar patterns of hip torque through scenario 2,4.

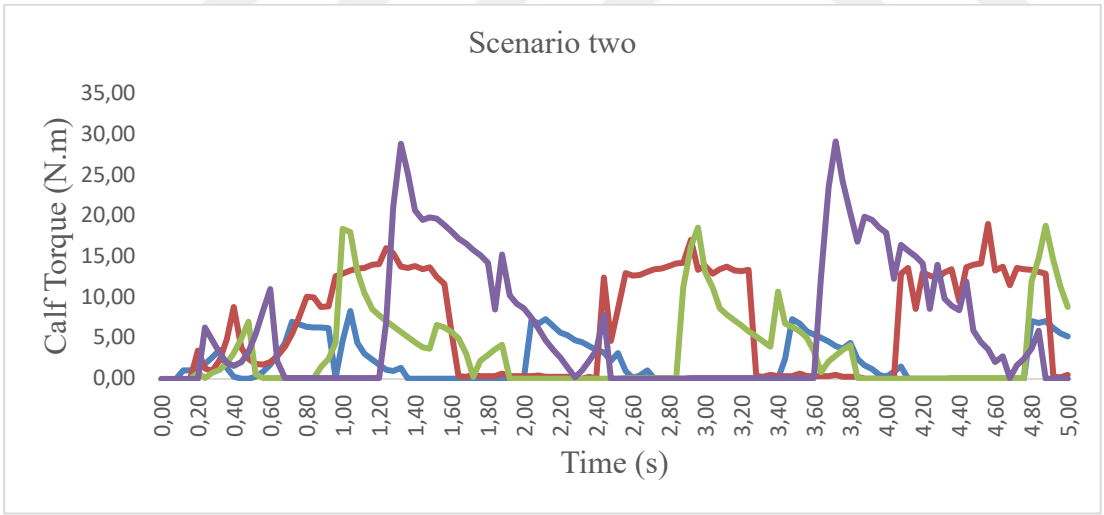


**Figure 5.8:** Similar patterns of calf torque through scenario 2,4.

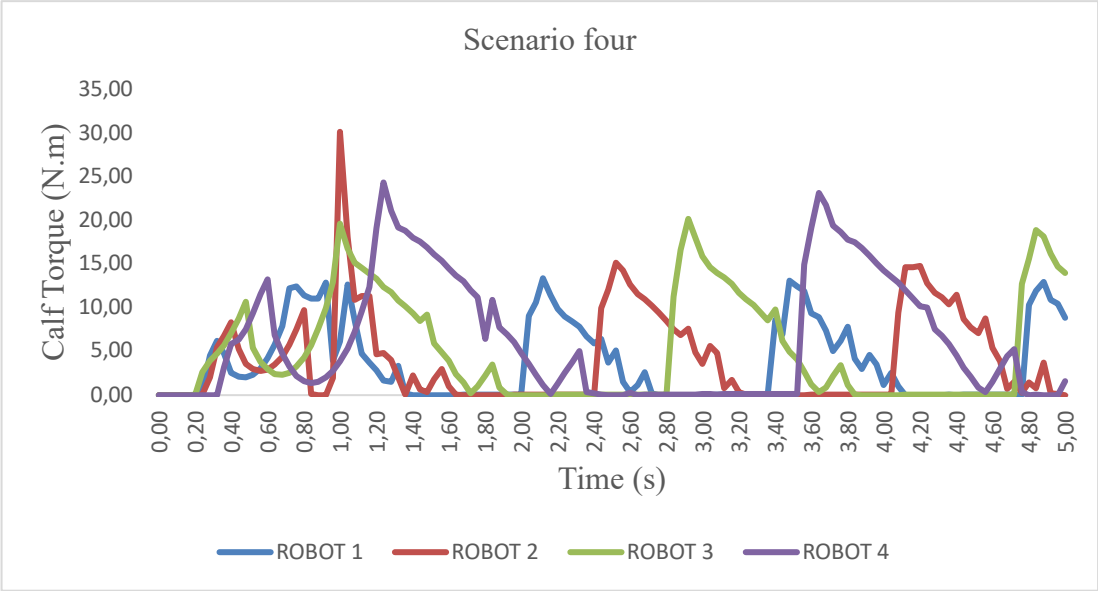


**Figure 5.8( continued):** Similar patterns of calf torque through scenario 2,4.

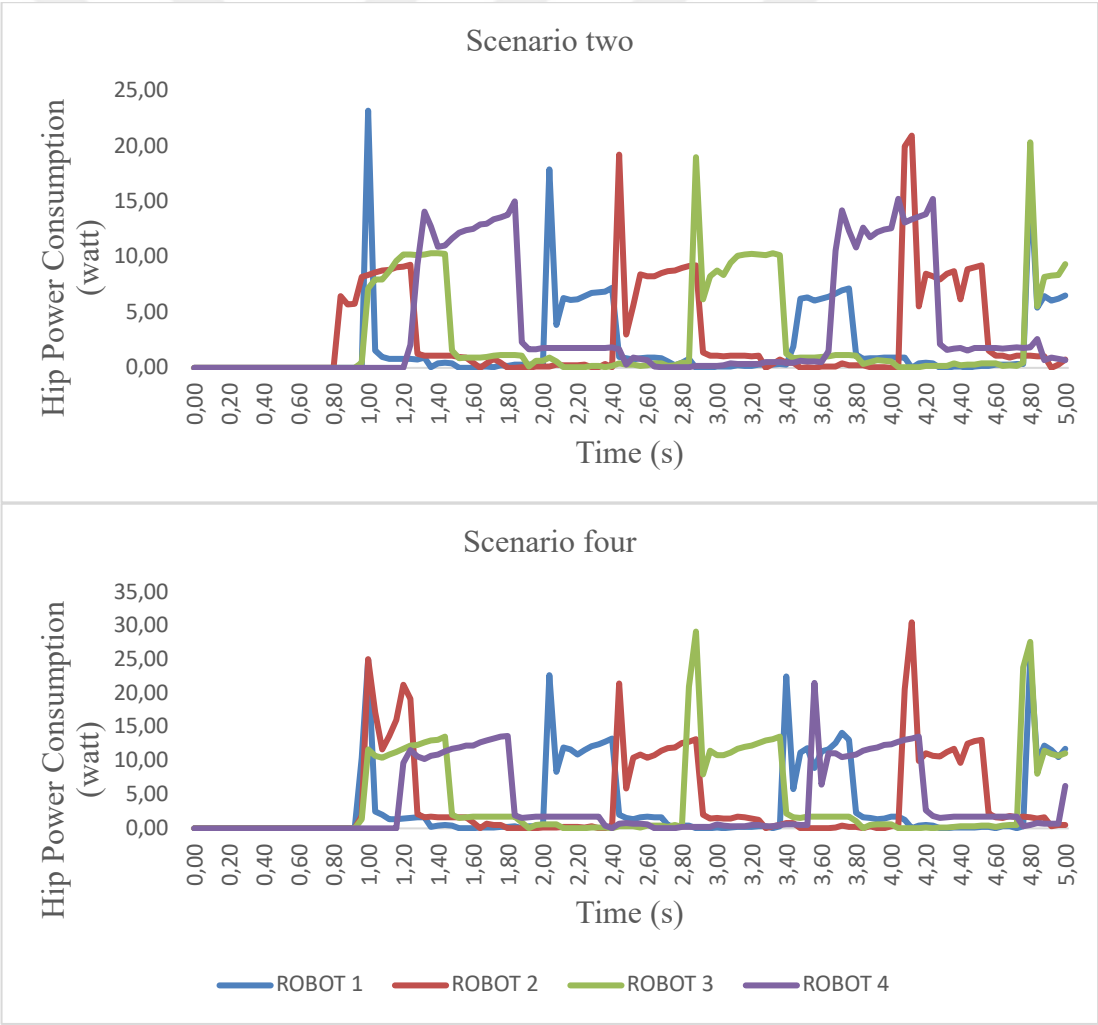


**Figure 5.9:** Similar patterns of hip power consumption through scenario 2,4.

We employed the same timing and positioning pattern of motors as in the second scenario, yet we were able to achieve identical linear velocities for the robots. This suggests that altering the dimensions of the arms and legs while not scaling the Torso has no significant effect on the pattern of hip torque, calf torque, hip power, and calf power of the robot, analogous to scenarios involving scaling of both the arms, legs, and the Torso. However, there is a notable difference in reaction forces between the end effector and the ground. While the Torso remains unscaled, the magnitude of the reaction forces remains constant, whereas in scenario two, we observe an increase in magnitudes. This difference is significant in the design and optimization of the arm, leg, and end effector to address the reaction forces, as depicted in Figure 5.11. Additionally, there is a considerable increase in the magnitude of hip torque, calf torque, hip power, and calf power in scenario four, akin to previous scenarios.

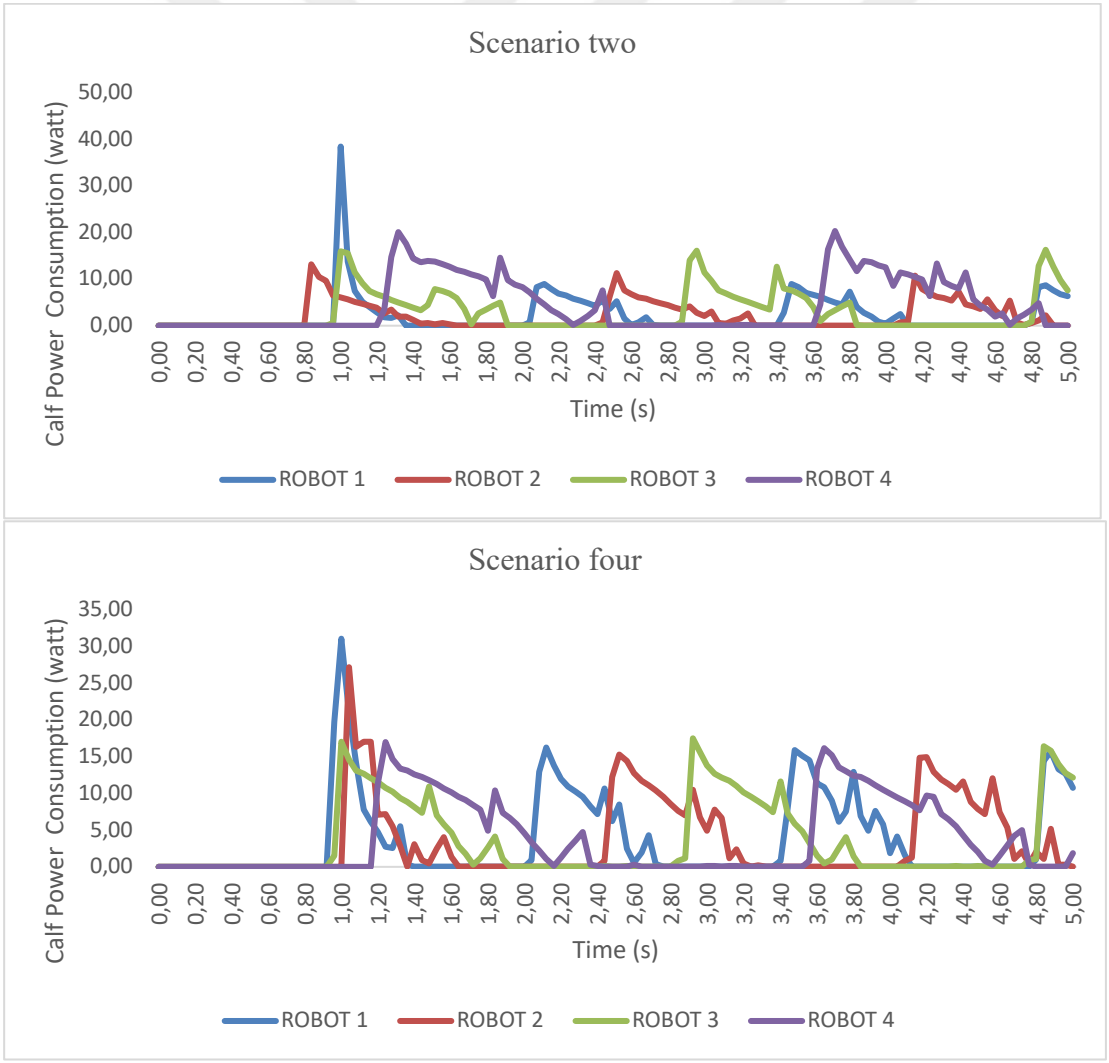


**Figure 5.10:** Similar patterns of calf power consumption through scenarios 2,4.

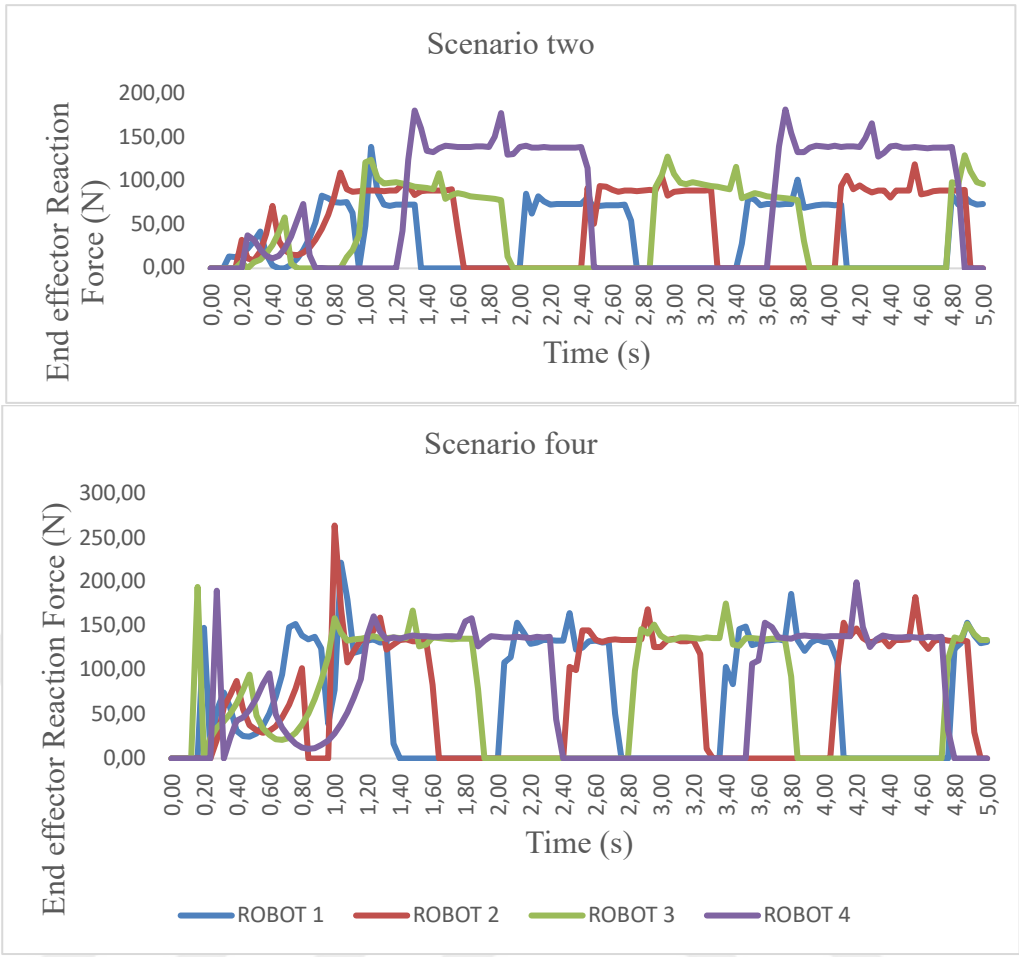


**Figure 5.11:** Patterns of end effector reaction forces through scenarios 2,4.

On the other hand, in scenario five, the starting and ending moments of the hip torque (Figure 5.12), calf torque (Figure 5.13), hip power (Figure 5.14), calf power (Figure 5.15), and reaction forces (Figure 5.16) on the end effector are consistent, whereas in other scenarios, they differ.

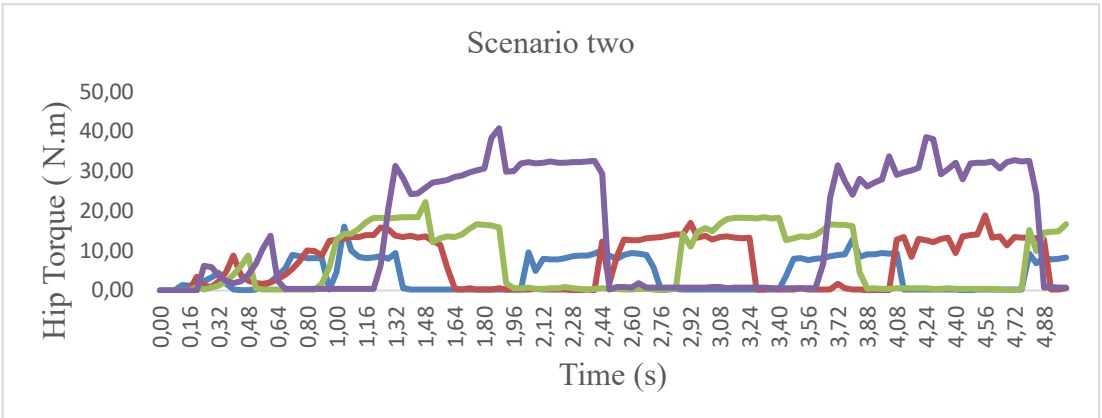


**Figure 5.12:** Hip torque through scenarios 2,5.

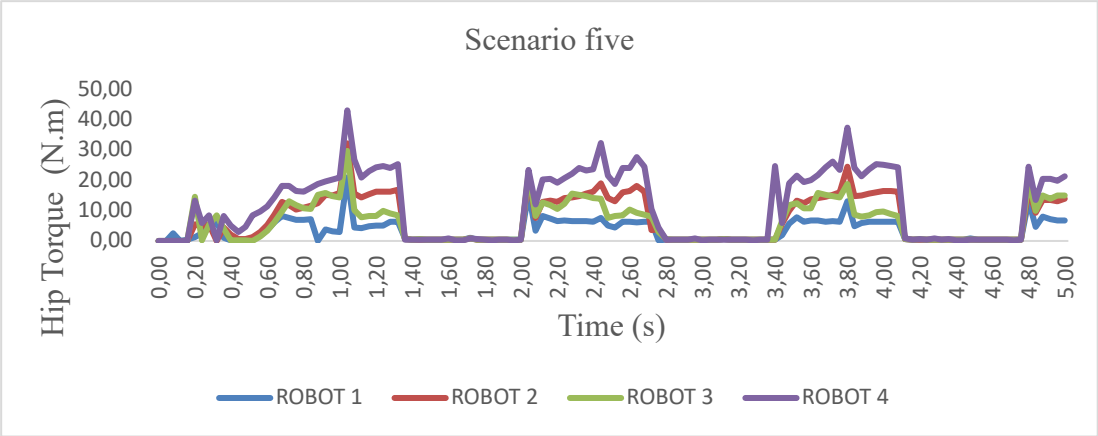


**Figure 5.12(continued):** Hip torque through scenarios 2,5.

There is a significant decrease in the magnitude of the mechanical parameters between the scenarios, especially in the largest robot. The total maximum magnitude of hip torque, calf torque, hip power, calf power, and reaction forces in robot four of scenario four is approximately 21 N.m, while the corresponding value for the same robot in scenario two is roughly 30 N.m. This demonstrates that the change in Torso size has a considerable impact on the hip torque, particularly in larger dimensions.

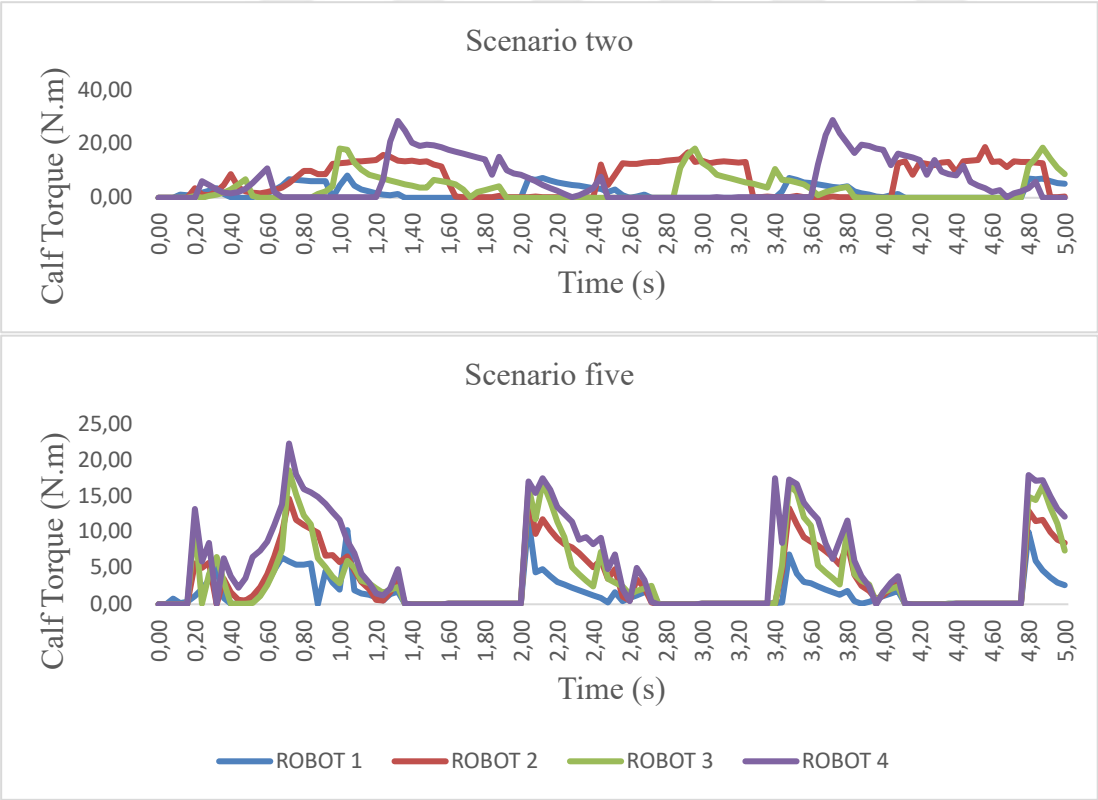


**Figure 5.13:** Calf torque through scenarios 2,5.

The positioning and timing of the calf and hip motors in scenario five are all the same, consistent with the pair working logic in motors two by two (Figure 5.17). This pattern

differs from the motor pattern observed in scenario two. This demonstrates that when scaling a quadruped robot while maintaining the same sizes for the arms and legs, we can utilize a single type of positioning and timing motor, considering the required torques and power consumption.

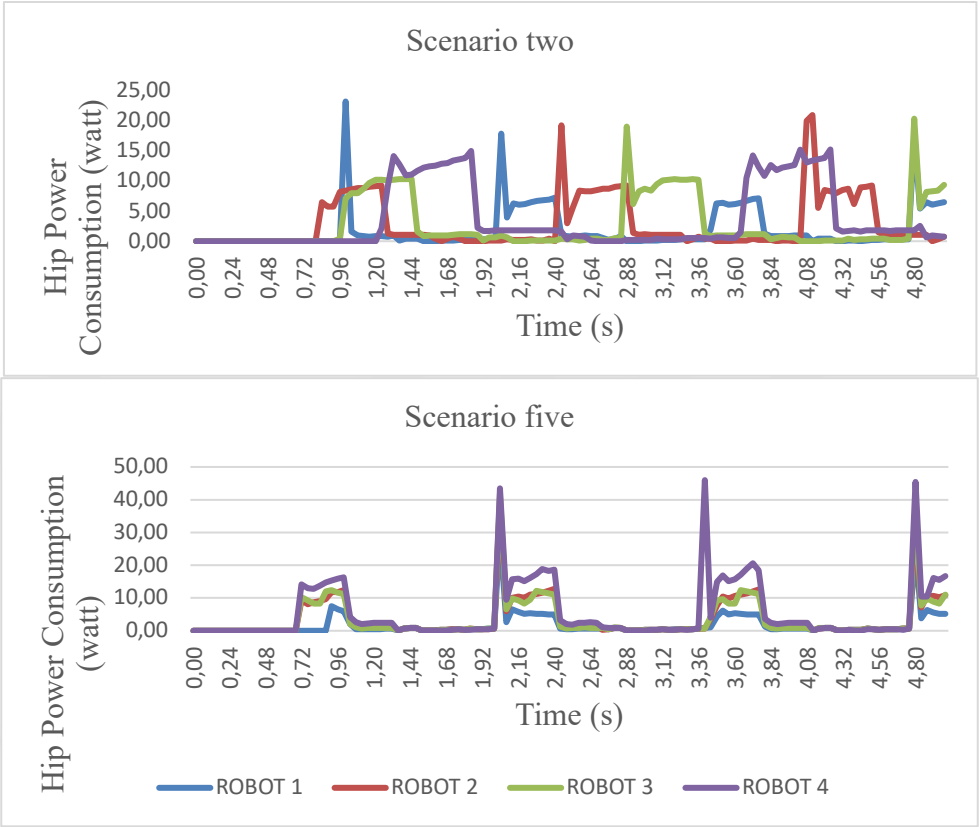


**Figure 5.14:** Hip power consumption through scenarios 2,5.

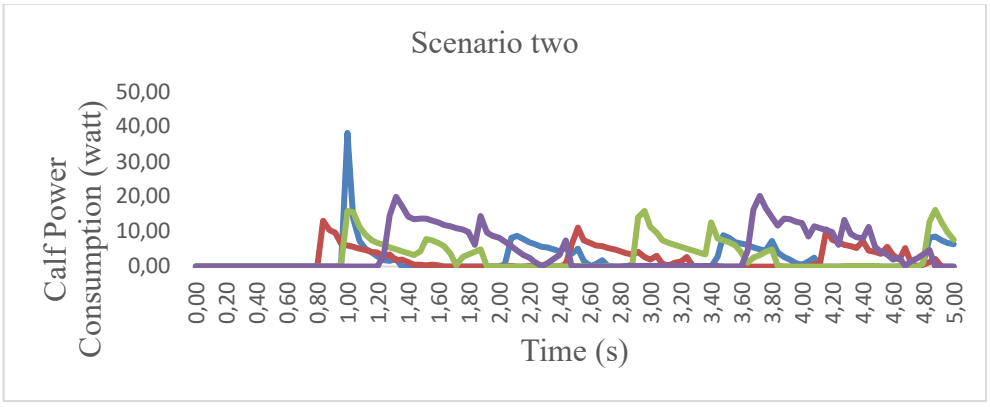


**Figure 5.15:** Calf power consumption through scenarios 2,5.

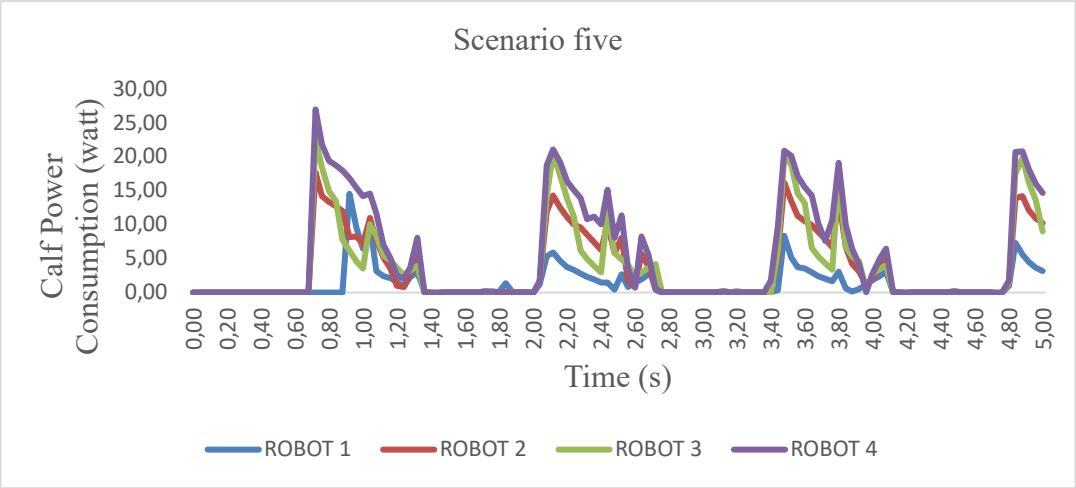


**Figure 5.15(continued):** Calf power consumption through scenarios 2,5.

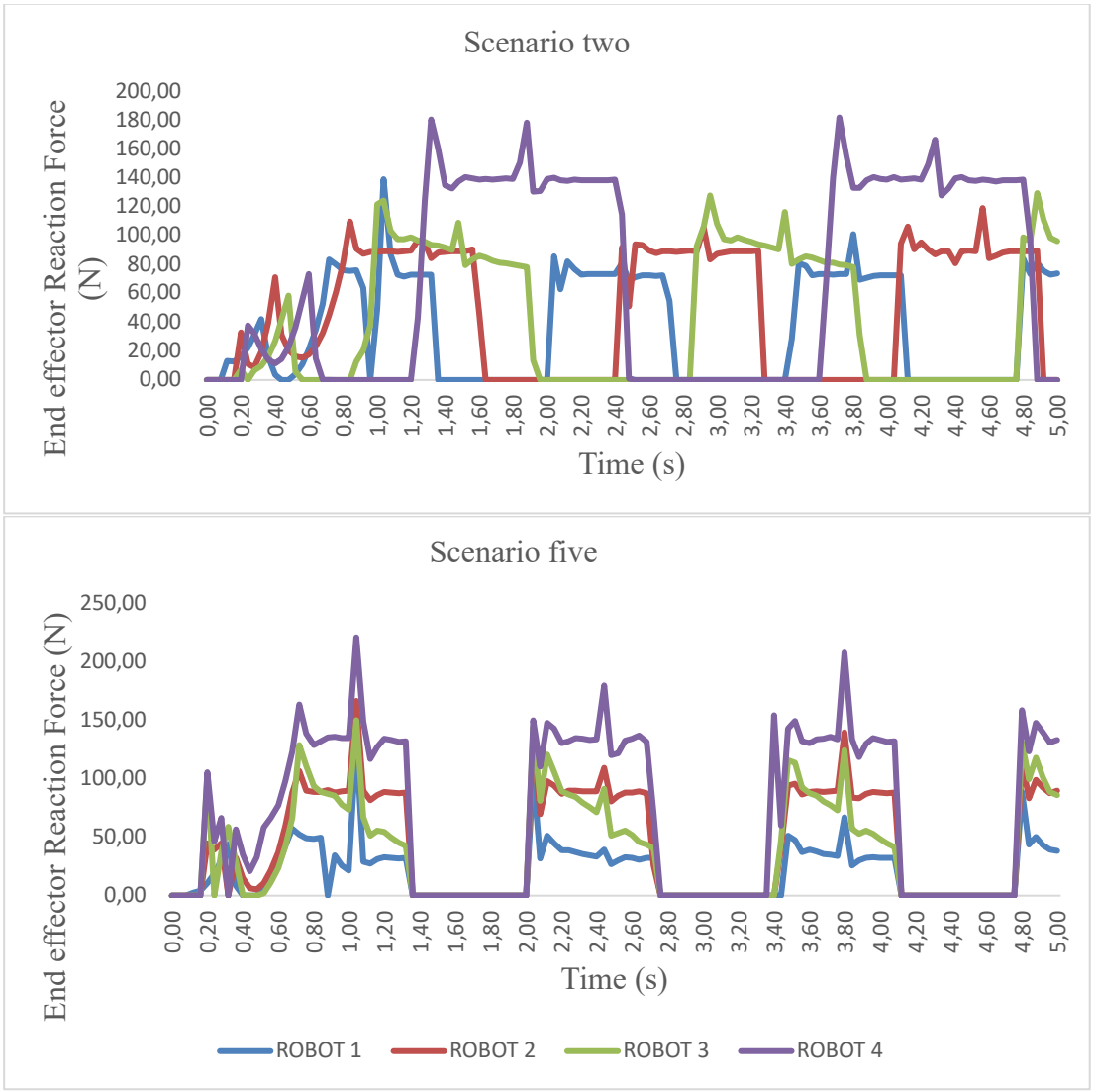


**Figure 5.16:** End effector reaction forces consumption through scenario 2,5.

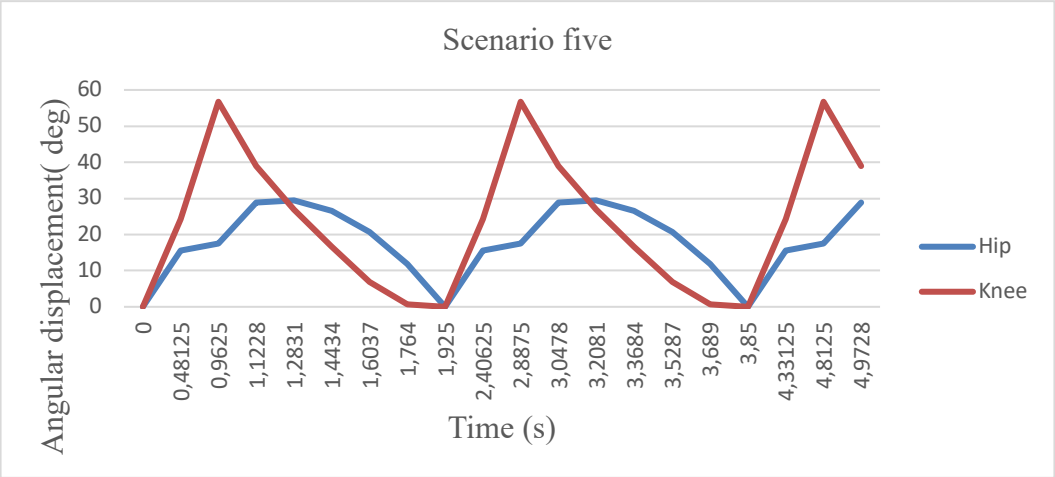


**Figure 5.17:** Angular displacement of the hip and torque of scenario five.

### 5.3 Mechanical Cost of Transport

The mechanical cost of transport can be calculated as seen in equation 3.1.

$$\text{MCOT} = \frac{\Sigma P}{w \times d}$$

where $P$ represents power consumption, $w$ is the mass being transported, typically measured in kilograms (kg), and $d$ denotes the distance traveled during locomotion, usually measured in meters (m). The total power consumption, usually measured in watts (W), is calculated through the total mechanical power expended during locomotion over the earned time interval. Since the power consumption data was provided in intervals of 0.04 seconds, we used the trapezoidal rule to approximate the area under the power consumption curve and then multiplied it by the time interval. The MCOT of the robots through the three scenarios with two example gear ratios are shown in Table 5.1.

**Table 5.1:** MCOT comparison in all scenarios.

| Gear ratio | Scenario | Robot 1 | Robot 2 | Robot 3 | Robot 4 |
|---|---|---|---|---|---|
| 8 | 1 | 0.83 | 0.935 | 0.72 | 0.82 |
| | 2 | 0.58 | 0.65 | 0.62 | 0.68 |

| | | | | | |
|---|---|---|---|---|---|
| | 3 | 0.76 | 0.7 | 0.75 | 0.66 |
| | 4 | 0.62 | 0.64 | 0.79 | 0.65 |
| | 5 | 0.36 | 0.67 | 0.59 | 0.67 |
| 6 | 1 | 1.1 | 1.24 | 0.96 | 1.1 |
| | 2 | 0.77 | 0.86 | 0.82 | 0.93 |
| | 3 | 1.01 | 0.93 | 1 | 0.88 |
| | 4 | 0.82 | 0.85 | 1.05 | 0.85 |
| | 5 | 0.48 | 0.89 | 0.76 | 0.89 |

**Tablo 5-1(continues):** MCOT comparison in all scenarios.

### 5.3.1 The comparison of the MCOT through the five scenarios

TCOT is the most common tool for measuring the energy efficiency of legged robots (Bhounsule, 2012), while MCOT does not consider the energy wastage within the electric motor. In this context, we focus on MCOT due to our mechanical design principles. Upon examining Table 4.1, we noted that MCOT rises as the gear ratio decreases. This is expected because a lower gear ratio results in higher total power consumption, thereby increasing MCOT. The influence of gear ratio on MCOT has been discussed in previous studies (Seok S. a., 2012) and is not the primary focus of this investigation. The subsequent comparisons is applicable for both given gear ratios.

#### 5.3.1.1 MCOT in scenarios one, two, and three

Upon reviewing Table 4.1, we observe a similar level of MCOT across all robots in each scenario, albeit with slight variations. Given that any alteration in MCOT can potentially impact energy efficiency, even minor discrepancies warrant consideration. We anticipated an increase in MCOT across scenarios one, two, and three from robots one to four because of the increase in the weight and dimension; however, this was not the case. From our perspective, this phenomenon can be attributed to the mechanical design's influence on MCOT. For instance, consider robot two in scenario one, which exhibits an MCOT of 0.935, surpassing that of robot one but falling short of robot four,

despite the latter's larger size and weight compared to robot two. Thus, mechanical design can significantly influence energy efficiency during scaling. Simulation results indicate that extending the length and height of the trajectory leads to a reduction in MCOT, with the decrease being more pronounced with trajectory lengthening.

#### 5.3.1.2 MCOT in scenarios four, and five

Scenarios four and five demonstrate that scaling the torso or the arms and legs does not significantly impact the MCOT compared to scenario two, except for robot five in scenario five. This suggests that a smaller torso coupled with longer arms and legs yields a superior MCOT. For example, the MCOT for robot one in scenario five is 0.36, whereas in scenario two, it is 0.58.

# 6. CONCLUSIONS AND RECOMMENDATIONS

Quadruped robots demonstrate invaluable capabilities for specialized tasks, particularly in disaster scenarios like earthquakes, where their mobility often surpasses that of fixed robots. However, modifying the dimensions of these robots significantly impacts their mechanical requirements and control systems. This study aimed to investigate and compare key mechanical parameters, including hip and calf torque, hip and calf power consumption, reaction forces between the end effector and the ground, and the mechanical cost of transport of scaled robots across five different scenarios. Our objective was to observe their effects on the dynamics of quadruped robots during scaling. Utilizing the motion analysis tool within SolidWorks, we conducted simulations involving a standard Unitree A1 quadruped robot walking on an even flat surface at a constant linear velocity of 250 meters per second. We observed that the behavioral patterns of the robots during scaling with various trajectory dimensions remained relatively consistent. However, the magnitude of these mechanical principles increased in each scenario due to the elongation of the torso, arms, and legs. Significant variations were noted in the angular velocity and displacement of the arms and legs, which directly correlated with the motors' performance. Thus, successful scaling of the robots during operations hinges on the motors' ability to meet maximum torque and power consumption requirements, while adapting to the necessary angular velocity. Our observations revealed a consistent cost of transport across scenarios, albeit with a decrease in the mechanical cost of transport (MCOT) as trajectory length and height increased. This finding underscores the impact of even minor differences in mechanical parameters on energy efficiency. These outcomes provide comprehensive insights into critical mechanical components, including joints, offering valuable references for various actuator architecture designs such as series elastics or QQDs. Importantly, these references are not limited to a singular type of actuator, thereby enhancing their applicability. Our findings elucidate a discernible pattern of torques, power consumptions, and reaction forces as the robot scales in size. In future research endeavors, we intend to leverage these fundamental data to develop a scalable control architecture with a focus on machine learning integration.

## REFERENCES


**Aceituno-Cabezas, B. a.-L.** (2017). Simultaneous contact, gait, and motion planning for robust multilegged locomotion via mixed-integer convex optimization. IEEE Robotics and Automation Letters, 2531--2538.

**Ananthanarayanan, A. a.** (2012). Towards a bio-inspired leg design for high-speed running. Bioinspiration \& biomimetics, 046005.

**Andrychowicz, O. M.** (2020). Learning dexterous in-hand manipulation. The International Journal of Robotics Research, 3--20.

**Apgar, T. a. (2018).** Fast Online Trajectory Optimization for the Bipedal Robot Cassie. Robotics: Science and Systems (s. 14). içinde Pittsburgh, Pennsylvania, USA.

**Azad, M. a.** (2015). Balance control strategy for legged robots with compliant contacts. 2015 IEEE International Conference on Robotics and Automation (ICRA) (s. 4391--4396). içinde IEEE.

**Bajracharya, M. a.** (2013). High fidelity day/night stereo mapping with vegetation and negative obstacle detection for vision-in-the-loop walking. 2013 IEEE/RSJ International Conference on Intelligent Robots and Systems (s. 3663--3670). içinde IEEE.

**Bazeille, S. a.** (2014). Quadruped robot trotting over irregular terrain assisted by stereo-vision. Intelligent Service Robotics, 67--77.

**Bellicoso, C. D.** (2017). Dynamic locomotion and whole-body control for quadrupedal robots. 2017 IEEE/RSJ International Conference on Intelligent Robots and Systems (IROS) (s. 3359--3365). içinde IEEE.

**Bellicoso, C. D.** (2018). Dynamic locomotion through online nonlinear motion optimization for quadrupedal robots. IEEE Robotics and Automation Letters, 2261--2268.

**Belter, D. a.** (2016). Adaptive motion planning for autonomous rough terrain traversal with a walking robot. Journal of Field Robotics, 337--370.

**Bhounsule, P. A.** (2012). Design and control of Ranger: an energy-efficient, dynamic walking robot. Adaptive Mobile Robotics (s. 441--448). World Scientific.

**Bledt, G. a.** (2017). Policy-regularized model predictive control to stabilize diverse quadrupedal gaits for the MIT cheetah. 2017 IEEE/RSJ International Conference on Intelligent Robots and Systems (IROS) (s. 4102--4109). içinde IEEE.

**Bledt, G. a.** (2018). Mit cheetah 3: Design and control of a robust, dynamic quadruped robot. 2018 IEEE/RSJ International Conference on Intelligent Robots and Systems (IROS) (s. 2245--2252). içinde IEEE.

**Boney, R. a.** (2020). RealAnt: An Open-Source Low-Cost Quadruped for Education and Research in Real-World Reinforcement Learning. arXiv preprint arXiv:2011.03085.

**Bosworth, W. a.** (2015). The mit super mini cheetah: A small, low-cost quadrupedal robot for dynamic locomotion. 2015 IEEE International Symposium on Safety, Security, and Rescue Robotics (SSRR) (s. 1--8). içinde IEEE.

**Bouman, A. a.-K.** (2020). Autonomous spot: Long-range autonomous exploration of extreme environments with legged locomotion. 2020 IEEE/RSJ International Conference on Intelligent Robots and Systems (IROS) (s. 2518--2525). içinde IEEE.

**Bouyarmane, K. a.** (2018). Quadratic programming for multirobot and task-space force control. IEEE Transactions on Robotics, 64--77.

**Carius, J. a.** (2018). Trajectory optimization with implicit hard contacts. IEEE Robotics and Automation Letters, 3316--3323.

**Chebotar, Y. a.** (2019). Closing the sim-to-real loop: Adapting simulation randomization with real world experience. 2019 International Conference on Robotics and Automation (ICRA) (s. 8973--8979). içinde IEEE.

**Coros, S. a.** (2009). Robust task-based control policies for physics-based characters. ACM SIGGRAPH Asia 2009 papers. içinde

**Coros, S. a.** (2010). Generalized biped walking control. ACM Transactions On Graphics (TOG), 1--9.

**Coros, S. a.** (2011). Locomotion skills for simulated quadrupeds. ACM Transactions on Graphics (TOG), 1--12.

**Dai, H. a.** (2014). Whole-body motion planning with centroidal dynamics and full kinematics. 2014 IEEE-RAS International Conference on Humanoid Robots (s. 295--302). içinde IEEE.

**De Lasa, M. a.** (2010). Feature-based locomotion controllers. ACM transactions on graphics (TOG), 1--10.

**Deits, R. a.** (2014). Footstep planning on uneven terrain with mixed-integer convex optimization. 2014 IEEE-RAS international conference on humanoid robots (s. 279--286). içinde IEEE.

**Di Carlo, J. a.** (2018). Dynamic locomotion in the mit cheetah 3 through convex model-predictive control. 2018 IEEE/RSJ international conference on intelligent robots and systems (IROS) (s. 1--9). içinde IEEE.

**Duan, Y. a.** (2016). Rl $\^{} 2$: Fast reinforcement learning via slow reinforcement learning. arXiv preprint arXiv:1611.02779.

**Endo, G. a.** (2005). Learning cpg sensory feedback with policy gradient for biped locomotion for a full-body humanoid. AAAI (s. 1267--1273). içinde

**Fahmi, S. a.** (2019). Passive whole-body control for quadruped robots: Experimental validation over challenging terrain. IEEE Robotics and Automation Letters, 2553--2560.

**Fahmi, S. a.** (2020). Stance: Locomotion adaptation over soft terrain. IEEE Transactions on Robotics, 443--457.

**Fankhauser, P. a.** (2018). Robust rough-terrain locomotion with a quadrupedal robot. 2018 IEEE International Conference on Robotics and Automation (ICRA) (s. 5761--5768). içinde IEEE.

**Farshidian, F. a.** (2017). An efficient optimal planning and control framework for quadrupedal locomotion. 2017 IEEE International Conference on Robotics and Automation (ICRA) (s. 93--100). içinde IEEE.

**Farshidian, F. a.** (2017). Real-time motion planning of legged robots: A model predictive control approach. 2017 IEEE-RAS 17th International Conference on Humanoid Robotics (Humanoids) (s. 577--584). içinde IEEE.

**Farshidian, F. a.** (2017). Robust whole-body motion control of legged robots. 2017 IEEE/RSJ International Conference on Intelligent Robots and Systems (IROS) (s. 4589--4596). içinde IEEE.

**Farshidian, F. a.** (2017). Sequential linear quadratic optimal control for nonlinear switched systems. IFAC-PapersOnLine, 1463--1469.

**Finn, C. a.** (2017). Model-agnostic meta-learning for fast adaptation of deep networks. International conference on machine learning (s. 1126--1135). içinde PMLR.

**Folkertsma, G. A.** (2012). Parallel stiffness in a bounding quadruped with flexible spine. 2012 IEEE/RSJ International Conference on Intelligent Robots and Systems (s. 2210--2215). içinde IEEE.

**Gangapurwala, S. a.** (2022). Rloc: Terrain-aware legged locomotion using reinforcement learning and optimal control. IEEE Transactions on Robotics, 2908--2927.

**Garc{\'\i}a-C{\'a}rdenas, F. a.** (2020). Charlotte: Low-cost open-source semi-autonomous quadruped robot. 2020 IEEE International Conference on Autonomous Robot Systems and Competitions (ICARSC) (s. 281--286). içinde IEEE.

**Gehring, C. a.** (2016). Practice makes perfect: An optimization-based approach to controlling agile motions for a quadruped robot. IEEE Robotics \& Automation Magazine, 34--43.

**Geyer, H. a.** (2003). Positive force feedback in bouncing gaits? Proceedings of the Royal Society of London. Series B: Biological Sciences, 2173--2183.

**Goswami, A.** (1999). Foot rotation indicator (FRI) point: A new gait planning tool to evaluate postural stability of biped robots. Proceedings 1999 IEEE international conference on robotics and automation (Cat. No. 99CH36288C) (s. 47--52). içinde IEEE.

**Grandia, R. a.** (2023). Perceptive locomotion through nonlinear model-predictive control. IEEE Transactions on Robotics.

**Griffin, R. J.** (2019). Footstep planning for autonomous walking over rough terrain. 2019 IEEE-RAS 19th international conference on humanoid robots (humanoids) (s. 9--16). içinde IEEE.

**Grimes, D. B.** (2006). Dynamic imitation in a humanoid robot through nonparametric probabilistic inference. Robotics: science and systems (s. 199--206). içinde Citeseer.

**Haarnoja, T. a.** (2018). Learning to walk via deep reinforcement learning. arXiv preprint arXiv:1812.11103.

**Haberland, M. a.** (2011). The effect of swing leg retraction on running energy efficiency. 2011 IEEE/RSJ International Conference on Intelligent Robots and Systems (s. 3957--3962). içinde IEEE.

**Hanna, J. a.** (2017). Grounded action transformation for robot learning in simulation. Proceedings of the AAAI Conference on Artificial Intelligence. içinde

**Heess, N. a.** (2017). Emergence of locomotion behaviours in rich environments. arXiv preprint arXiv:1707.02286.

**Henze, B. a.** (2016). Passivity-based whole-body balancing for torque-controlled humanoid robots in multi-contact scenarios. The International Journal of Robotics Research, 1522--1543.

**Henze, B. a.** (2017). Multi-contact balancing of humanoid robots in confined spaces: Utilizing knee contacts. 2017 IEEE/RSJ International Conference on Intelligent Robots and Systems (IROS) (s. 697--704). içinde IEEE.

**Henze, B. a.-G.-S.** (2018). Passivity analysis and control of humanoid robots on movable ground. IEEE Robotics and Automation Letters, 3457--3464.

**Hooks, J. a.** (2020). Alphred: A multi-modal operations quadruped robot for package delivery applications. IEEE Robotics and Automation Letters, 5409--5416.

**Hurst, J. W.** (2010). The actuator with mechanically adjustable series compliance. IEEE Transactions on Robotics, 597--606.

**Hutter, M. a.** (2012). StarlETH: A compliant quadrupedal robot for fast, efficient, and versatile locomotion. Adaptive mobile robotics (s. 483--490). içinde World Scientific.

**Hwangbo, J. a.** (2019). Learning agile and dynamic motor skills for legged robots. Science Robotics, eaau5872.

**Iida, F. a.** (2005). Exploiting body dynamics for controlling a running quadruped robot. ICAR'05. Proceedings., 12th International Conference on Advanced Robotics, 2005. (s. 229--235). içinde IEEE.

**Jenelten, F. a.** (2020). Perceptive locomotion in rough terrain--online foothold optimization. IEEE Robotics and Automation Letters, 5370--5376.

**Jenelten, F. a.** (2022). TAMOLS: Terrain-aware motion optimization for legged systems. IEEE Transactions on Robotics, 3395--3413.

**Kalakrishnan, M. a.** (2010). Fast, robust quadruped locomotion over challenging terrain. 2010 IEEE International Conference on Robotics and Automation (s. 2665--2670). içinde IEEE.

**Katz, B. a.** (2019). Mini cheetah: A platform for pushing the limits of dynamic quadruped control. 2019 international conference on robotics and automation (ICRA) (s. 6295--6301). içinde IEEE.

**Katz, H., and Rees** (2021). W. "Quadruped robot design: A survey." International Journal of Robotics Research (2021).

**Khan, H. a.** (2015). Development of the lightweight hydraulic quadruped robot—MiniHyQ. 2015 IEEE international conference on technologies for practical robot applications (TePRA) (s. 1--6). içinde IEEE.

**Kim, D. a.** (2020). Vision aided dynamic exploration of unstructured terrain with a small-scale quadruped robot. 2020 IEEE International Conference on Robotics and Automation (ICRA) (s. 2464--2470). içinde IEEE.

**Kim, J. a.-J.** (2021). Design and control of a open-source, low cost, 3D printed dynamic quadruped robot. Applied Sciences, 3762.

**Kim, S. a.** (2009). Stable whole-body motion generation for humanoid robots to imitate human motions. 2009 IEEE/RSJ International Conference on Intelligent Robots and Systems (s. 2518--2524). içinde IEEE.

**Koenemann, J. a.** (2014). Real-time imitation of human whole-body motions by humanoids. 2014 IEEE International Conference on Robotics and Automation (ICRA) (s. 2806--2812). içinde IEEE.

**Kohl, N. a.** (2004). Policy gradient reinforcement learning for fast quadrupedal locomotion. IEEE International Conference on Robotics and Automation, 2004. Proceedings. ICRA'04. 2004 (s. 2619--2624). içinde IEEE.

**Kolter, J. Z.** (2008). A control architecture for quadruped locomotion over rough terrain. 2008 IEEE International Conference on Robotics and Automation (s. 811--818). içinde IEEE.

**Kweon, I.-S. a.** (1989). Terrain mapping for a roving planetary explorer. IEEE International Conference on Robotics and Automation (s. 997--1002). içinde IEEE.

**Lee, J. a.** (2020). Learning quadrupedal locomotion over challenging terrain. Science robotics, eabc5986.

**Lee, S. a.** (2019). Scalable muscle-actuated human simulation and control. ACM Transactions On Graphics (TOG), 1--13.

**Lee, Y. a.** (2010). Data-driven biped control. ACM SIGGRAPH 2010 papers (s. 1--8). içinde

**Liu, F. a.** (2010). Gait evolving method of quadruped robot using zero-moment point trajectory planning. Jiqiren(Robot), 398--404.

**Liu, L. a.** (2016). Guided learning of control graphs for physics-based characters. ACM Transactions on Graphics (TOG), 1--14.

**Liu, L. a.** (2018). Learning basketball dribbling skills using trajectory optimization and deep reinforcement learning. ACM Transactions on Graphics (TOG), 1--14.

**Lowrey, K. a.** (2018). Reinforcement learning for non-prehensile manipulation: Transfer from simulation to physical system. 2018 IEEE International Conference on Simulation, Modeling, and Programming for Autonomous Robots (SIMPAR) (s. 35--42). içinde IEEE.

**Maes, L. D.** (2008). Steady locomotion in dogs: temporal and associated spatial coordination patterns and the effect of speed. Journal of Experimental Biology, 138--149.

**Magana, O. A.** (2019). Fast and continuous foothold adaptation for dynamic locomotion through cnns. IEEE Robotics and Automation Letters, 2140--2147.

**Marcucci, T. a.** (2017). Approximate hybrid model predictive control for multi-contact push recovery in complex environments. IEEE.

**Mastalli, C. a.** (2015). On-line and on-board planning and perception for quadrupedal locomotion. 2015 IEEE International Conference on Technologies for Practical Robot Applications (TePRA) (s. 1--7). içinde IEEE.

**Mastalli, C. a.** (2020). Motion planning for quadrupedal locomotion: Coupled planning, terrain mapping, and whole-body control. IEEE Transactions on Robotics, 1635--1648.

**Mastalli, C. a.** (2022). Agile maneuvers in legged robots: a predictive control approach. arXiv preprint arXiv:2203.07554.

**Meduri, A. a.** (2023). Biconmp: A nonlinear model predictive control framework for whole body motion planning. IEEE Transactions on Robotics, 905--922.

**Melon, O. a.** (2020). Reliable trajectories for dynamic quadrupeds using analytical costs and learned initializations. 2020 IEEE International Conference on Robotics and Automation (ICRA) (s. 1410--1416). içinde IEEE.

**Miki, T. a.** (2022). Learning robust perceptive locomotion for quadrupedal robots in the wild. Science Robotics, eabk2822.

**Miura, H. a.** (1984). Dynamic walk of a biped. The International Journal of Robotics Research, 60--74.

**Mordatch, I. a.** (2012). Discovery of complex behaviors through contact-invariant optimization. ACM Transactions on Graphics (ToG), 1--8.

**Muico, U. a.** (2009). Contact-aware nonlinear control of dynamic characters. ACM SIGGRAPH 2009 papers (s. 1--9). içinde

**Nagabandi, A. a.** (2018). Learning to adapt in dynamic, real-world environments through meta-reinforcement learning. arXiv preprint arXiv:1803.11347.

**Nakaoka, S. a.** (2003). Generating whole body motions for a biped humanoid robot from captured human dances. 2003 IEEE International Conference on Robotics and Automation (Cat. No. 03CH37422) (s. 3905--3910). içinde IEEE.

**Neunert, M. a.** (2018). Whole-body nonlinear model predictive control through contacts for quadrupeds. IEEE Robotics and Automation Letters, 1458--1465.

**Orin, D. E.-H.** (2013). Centroidal dynamics of a humanoid robot. Autonomous robots, 161--176.

**Pardo, D. a.** (2017). Hybrid direct collocation and control in the constraint-consistent subspace for dynamic legged robot locomotion. Robotics: Science and Systems. içinde

**Park, H.-W. a.** (2017). High-speed bounding with the MIT Cheetah 2: Control design and experiments. The International Journal of Robotics Research, 167--192.

**Peng, X. B.** (2016). Terrain-adaptive locomotion skills using deep reinforcement learning. ACM Transactions on Graphics (TOG), 1--12.

**Peng, X. B.** (2018). Deepmimic: Example-guided deep reinforcement learning of physics-based character skills. ACM Transactions On Graphics (TOG), 1--14.

**Peng, X. B.** (2018). Sfv: Reinforcement learning of physical skills from videos. ACM Transactions On Graphics (TOG), 1--14.

**Peng, X. B.** (2018). Sim-to-real transfer of robotic control with dynamics randomization. 2018 IEEE international conference on robotics and automation (ICRA) (s. 3803--3810). içinde IEEE.

**Peng, X. B.-W.** (2020). Learning agile robotic locomotion skills by imitating animals. arXiv preprint arXiv:2004.00784.

**Pinto, L. a.** (2017). Robust adversarial reinforcement learning. International Conference on Machine Learning (s. 2817--2826). içinde PMLR.

**Pollard, N. S.** (2002). Adapting human motion for the control of a humanoid robot. Proceedings 2002 IEEE international conference on robotics and automation (Cat. No. 02CH37292) (s. 1390--1397). içinde IEEE.

**Ponton, B. a.** (2018). On time optimization of centroidal momentum dynamics. 2018 IEEE International Conference on Robotics and Automation (ICRA) (s. 5776--5782). içinde IEEE.

**Posa, M. a.** (2014). A direct method for trajectory optimization of rigid bodies through contact. The International Journal of Robotics Research, 69--81.

**Raibert, M. a.** (2008). Bigdog, the rough-terrain quadruped robot. IFAC Proceedings Volume, 10822--10825.

**Raibert, M. H.** (1984). Hopping in legged systems—modeling and simulation for the two-dimensional one-legged case. IEEE Transactions on Systems, Man, and Cybernetics, 451--463.

**Raibert, M. H.** (1986). Legged robots that balance. MIT press.

**Ramos, J. a.** (2018). Facilitating model-based control through software-hardware co-design. 2018 IEEE International Conference on Robotics and Automation (ICRA) (s. 566--572). içinde IEEE.

**Rathod, N. a.** (2021). Model predictive control with environment adaptation for legged locomotion. IEEE Access, 145710--145727.

**Ruina, A. a.** (2005). A collisional model of the energetic cost of support work qualitatively explains leg sequencing in walking and galloping, pseudo-

elastic leg behavior in running and the walk-to-run transition. Journal of theoretical biology, 170--192.

**Rusu, A. A.** (2017). Sim-to-real robot learning from pixels with progressive nets. Conference on robot learning (s. 262--270). içinde PMLR.

**Sadeghi, F. a.** (2016). Cad2rl: Real single-image flight without a single real image. arXiv preprint arXiv:1611.04201.

**Salameh, Z. a.** (2009). Advanced lithium polymer batteries. 009 IEEE Power \& Energy Society General Meeting (s. 1--5). içinde IEEE.

**Sardain, P. a.** (2004). Forces acting on a biped robot. Center of pressure-zero moment point. IEEE Transactions on Systems, Man, and Cybernetics-Part A: Systems and Humans, 630--637.

**Seok, S. a.** (2012). Actuator design for high force proprioceptive control in fast legged locomotion. 2012 IEEE/RSJ International Conference on Intelligent Robots and Systems (s. 1970--1975). içinde IEEE.

**Seok, S. a.** (2014). Design principles for energy-efficient legged locomotion and implementation on the MIT cheetah robot. Ieee/asme transactions on mechatronics, 1117--1129.

**Sombolestan, M. a.** (2021). Adaptive force-based control for legged robots. 2021 IEEE/RSJ International Conference on Intelligent Robots and Systems (IROS) (s. 7440--7447). içinde IEEE.

**Spr{\"o}witz, A. a.** (2013). Towards dynamic trot gait locomotion: Design, control, and experiments with Cheetah-cub, a compliant quadruped robot. The International Journal of Robotics Research, 932--950.

**Suleiman, W. a.-P.** (2008). On human motion imitation by humanoid robot. 2008 IEEE International conference on robotics and automation (s. 2697--2704). içinde IEEE.

**Sun, T. a.** (2020). Small-sized reconfigurable quadruped robot with multiple sensory feedback for studying adaptive and versatile behaviors. Frontiers in neurorobotics, 14.

**Tan, J. a.** (2016). Simulation-based design of dynamic controllers for humanoid balancing. 2016 IEEE/RSJ International Conference on Intelligent Robots and Systems (IROS) (s. 2729--2736). içinde IEEE.

**Tan, J. a.** (2018). Sim-to-real: Learning agile locomotion for quadruped robots. arXiv preprint arXiv:1804.10332.

**Tedrake, R. a.** (2004). Stochastic policy gradient reinforcement learning on a simple 3D biped. 2004 IEEE/RSJ International Conference on Intelligent Robots and Systems (IROS)(IEEE Cat. No. 04CH37566) (s. 2849--2854). içinde IEEE.

**Tedrake, R. a.-f.** (2004). Actuating a simple 3D passive dynamic walker. IEEE International Conference on Robotics and Automation, 2004. Proceedings. ICRA'04. 2004 (s. 4656--4661). IEEE.

**Tobin, J. a.** (2017). Domain randomization for transferring deep neural networks from simulation to the real world. 2017 IEEE/RSJ international conference on intelligent robots and systems (IROS) (s. 23--30). içinde IEEE.

**Tonneau, S. a.** (2018). An efficient acyclic contact planner for multiped robots. IEEE Transactions on Robotics, 586--601.

**Torres, D. a.** (2015). Regenerative braking of BLDC motors. High-Perfor-mance Microcontroller Division Microchip Technology Inc.

**Tranzatto, M. a.** (2022). Cerberus: Autonomous legged and aerial robotic exploration in the tunnel and urban circuits of the darpa subterranean challenge. arXiv preprint arXiv:2201.07067.

**Vasilopoulos, V. a.** (2018). Monopod hopping on compliant terrains. Robotics and Autonomous Systems, 13--26.

**Villarreal, O. a.** (2020). Mpc-based controller with terrain insight for dynamic legged locomotion. 2020 IEEE International Conference on Robotics and Automation (ICRA) (s. 2436--2442). içinde IEEE.

**Wermelinger, M. a.** (2016). Navigation planning for legged robots in challenging terrain. 2016 IEEE/RSJ International Conference on Intelligent Robots and Systems (IROS) (s. 1184--1189). içinde IEEE.

**Weyand, P. G.** (2000). Faster top running speeds are achieved with greater ground forces not more rapid leg movements. Journal of applied physiology.

**Williamson, M. M.** (1995). Series elastic actuators.

**Winkler, A. W.** (2018). Gait and trajectory optimization for legged systems through phase-based end-effector parameterization. IEEE Robotics and Automation Letters, 1560--1567.

**Wolf, S. a.** (2008). A new variable stiffness design: Matching requirements of the next robot generation. 2008 IEEE International Conference on Robotics and Automation (s. 1741--1746). içinde IEEE.

**Xie, Z. a.** (2020). Learning locomotion skills for cassie: Iterative design and sim-to-real. Conference on Robot Learning (s. 317--329). içinde PMLR.

**Yamane, K. a.** (2010). Controlling humanoid robots with human motion data: Experimental validation. 2010 10th IEEE-RAS International Conference on Humanoid Robots (s. 504--510). içinde IEEE.

**Yin, K. a.** (2007). Simbicon: Simple biped locomotion control. ACM Transactions on Graphics (TOG), 105--es.

**Yoong, M. a.** (2010). Studies of regenerative braking in electric vehicle. 2010 IEEE conference on sustainable utilization and development in engineering and technology (s. 40--45). içinde IEEE.

**Yu, W. a.** (2021). Visual-locomotion: Learning to walk on complex terrains with vision. 5th Annual Conference on Robot Learning. içinde

**Zhao, Q. a.** (2012). Embodiment enables the spinal engine in quadruped robot locomotion. 2012 IEEE/RSJ International Conference on Intelligent Robots and Systems (s. 2449--2456). içinde IEEE.

**Zucker, M. a.** (2013). Chomp: Covariant hamiltonian optimization for motion planning. The International journal of robotics research, 1164--1193

**CURRICULUM VITAE**

**Name Surname** **: Faraz Rahvar**

**EDUCATION** **:**

- **B.Sc.** **:** 2017, Urmia University, Engineering Faculty, Mechanical Engineering Department

**PROFESSIONAL EXPERIENCE AND REWARDS:**

- Winner of the research grant for BAP( Bilimsel Araştırma Projeleri) Projects totaling 30,000 Turkish liras at Istanbul Technical University.
- Ranked within the top five percent of candidates admitted in the Entrance Exam (Konkur) of Iranian Universities. ( 5600th out of 100,000 people)
- Winner of the Young Entrepreneur Award in the field of the oil and gas industry of Iran
- Winner of the Top Young Manufacturers Award in the oil and gas industry of Iran

**PUBLICATIONS, PRESENTATIONS AND PATENTS ON THE THESIS:**

- **Faraz Rahvar, A. Y.** (2024). Size Matters: Exploring the Impact of Scaling on Quadruped Robot Dynamics. 25th Annual Conference Towards Autonomous Robotic Systems (TAROS 2024). London: TAROS 2024